Stabilized Finite Element Methods for Feedback Control of Convection Diffusion Equations

Denise A. Krueger

Dissertation submitted to the Faculty of the
Virginia Polytechnic Institute and State University
in partial fulfillment of the requirements for the degree of

Doctor of Philosophy
in
Mathematics

Belinda B. King, Chair
Jeff Borggaard
John A. Burns
Traian Iliescu
Lizette Zietsman

July 20, 2004
Blacksburg, Virginia

Keywords: Linear Quadratic Regulator Problems, Non-normal, Convection-Diffusion Equation, Stabilized Finite Elements

Stabilized Finite Element Methods for Feedback Control of Convection Diffusion Equations

Denise A. Krueger

ABSTRACT

We study the behavior of numerical stabilization schemes in the context of linear quadratic regulator (LQR) control problems for convection diffusion equations. The motivation for this effort comes from the observation that when linearization is applied to fluid flow control problems the resulting equations have the form of a convection diffusion equation. This effort is focused on the specific problem of computing the feedback functional gains that are the kernels of the feedback operators defined by solutions of operator Riccati equations. We develop a stabilization scheme based on the Galerkin Least Squares (GLS) method and compare this scheme to the standard Galerkin finite element method. We use cubic B-splines in order to keep the higher order terms that occur in GLS formulation. We conduct a careful numerical investigation into the convergence and accuracy of the functional gains computed using stabilization. We also conduct numerical studies of the role that the stabilization parameter plays in this convergence. Overall, we discovered that stabilization produces much better approximations to the functional gains on coarse meshes than the unstabilized method and that adjustments in the stabilization parameter greatly effects the accuracy and convergence rates. We discovered that the optimal stabilization parameter for simulation and steady state analysis is not necessarily optimal for solving the Riccati equation that defines the functional gains. Finally, we suggest that the stabilized GLS method might provide good initial values for iterative schemes on coarse meshes.

This work was funded in part by the Air Force Office of Scientific Research under grant number F49620-03-1-0243 and the National Science Foundation under grant DMS-0072629.

Dedication

To Justin, Laura, and Sara

With Love and Appreciation

Acknowledgments

To my advisor, Dr. Belinda B. King: Thank you for the guidance, support, understanding and opportunities you have given me. Your inspiration has forever changed my life, opening the doors to a world full of possibilities.

To my committee members and other math department faculty: Thank you for the time and knowledge you have shared with me either in the classroom or in research discussions. In particular, thank you to Dr. John Burns, your endless patience and instruction, in English as well as Math, made this dissertation possible. Also my sincere appreciation to Dr. Lizette Zietsman. I will always treasure your friendship, wisdom, and humor. Dankie. Dr. Jeff Borggaard and Dr. Traian Iliescu, your support and expertise is greatly valued.

To Dr. Jesus M. de la Garza: Where do I begin ... there are not enough words (even in Spanish) to express my sincere gratitude to you. Your friendship, guidance, encouragement, endless support and confidence in me are priceless. Muchos gracias.

To my family: Mom and Dad - Thank you for all you have done. The opportunities, education and upbringing you provided, along with the morals and values you instilled in me, were instrumental in my achieving this dream. Mark, Alan, Brian, and Maureen, thank you for the influence you have had on my life.

To my friends, swim family and coaches: This journey would not have been possible with out your help. The support, encouragement and assistance I have received from you has been overwhelming. Thank you.

To Justin, Laura, Sara: Thank you for being you. I would never have accomplished this if you were not who you are. Your love, support, encouragement and willingness to help out were invaluable throughout this process. You are three great kids.

Above all, thank you to my God, who makes all things possible.

Contents

List of Figures

List of Tables

Chapter 1

Introduction

During the past ten years considerable attention has been devoted to the problem of computing feedback controllers for fluid flow problems. One approach is to linearize the problem about a given laminar flow and then use linear feedback to control the flow near this equilibrium. This approach has been the subject of numerous studies (see [5], [10], [37], [38], [39]). Yet very little work has been done on the numerical problem of developing accurate methods for computing the feedback laws for the resulting linearized system.

There are at least two issues that one must deal with in order to analyze numerical methods when applied to certain flow control problems. First, the linearized equation is often convection dominated and it is well known that standard finite element Galerkin methods are not necessarily suitable even for the simulation problem. However, for straight simulation, numerical methods based on upwind and stabilization techniques have been developed specifically to deal with convection dominated problems. On the other hand, it is not at all clear that such schemes are appropriate for solving feedback control problems.

The second issue has to do with "dual convergence" since the linearized equations are known to be highly non-normal (see [4], [5], [6], [13], [37], [38], [39], [49] and [50]). As noted in [13], non-normal control systems require that more attention be paid to the problem of construction of numerical algorithms that approximate the dual system. In addition, in order to assure convergence of the feedback control laws, numerical schemes need to preserve exponential stabilizability (POES) uniformly (see [8] and [13]). In [8], Banks and Kunisch developed a general convergence theory for linear quadratic optimal control of parabolic

problems and proved that standard finite element schemes yield convergent feedback control laws. However, their numerical results were limited to the self-adjoint heat equation. Although standard finite element schemes work well in this symmetric case, these methods converge too slowly to be useful in convection dominated problems.

Recently, Vugrin [52] studied this question for the 1D convection diffusion control problem. Vugrin's dissertation focused on the use of re-norming and pre-conditioners to improve the convergence of the control laws. These approaches were based on the fact that even though the linear convection diffusion operator is not self-adjoint, there is a simple transformation that yields an equivalent self-adjoint system. This observation allowed Vugrin to establish convergence, but does not yield a practical numerical algorithm since the resulting transformed control problem is extremely ill-conditioned.

Collis and Heinkenschloss (see [21]),have recently studied the effect of the streamline upwind/Petrov Galerkin stabilized finite element method on the discretization of optimal control problems governed by the advection diffusion equation. The goal of this effort, however, is to develop a computational method for feedback control that converges faster and is less ill-conditioned. We consider a specific stabilization scheme based on a GLS method discussed in reference [42].

To provide motivation for studying convection dominated problems we briefly describe a channel flow control problem examined in [5], [38], [39] and [40]. We use this example to illustrate the structure of a typical linearization of a flow problem and to set the stage for formulating a feedback control problem for fluid flow systems.

1.1 Channel Flow Problem

Consider the problem where an incompressible fluid is flowing in a channel, Ω, defined by two parallel plates where $\Omega = (-\infty, \infty) \times (-1, 1) \times (-\infty, \infty)$. Let $p(t, x, y, z)$ denote the pressure and $\vec{u} = [u(t, x, y, z), v(t, x, y, z), w(t, x, y, z)]^T$ denote the three velocity components of the flow for $(x, y, z) \in \Omega$. The pressure and velocity fields are governed by the 3D Navier-Stokes

equations given by

$$\frac{\partial \vec{u}}{\partial t} + (\vec{u} \cdot \nabla)\, \vec{u} = -\nabla p + \frac{1}{\mathrm{Re}} \Delta \vec{u}, \tag{1.1}$$

$$\nabla \cdot \vec{u} = 0, \tag{1.2}$$

where Re is the Reynolds number. The system (1.1)-(1.2) is the starting point for most studies and has the explicit form

$$\frac{\partial u}{\partial t} + u\frac{\partial u}{\partial x} + v\frac{\partial u}{\partial y} + w\frac{\partial u}{\partial z} = \frac{1}{\mathrm{Re}}\Delta u - \frac{\partial p}{\partial x}, \tag{1.3}$$

$$\frac{\partial v}{\partial t} + u\frac{\partial v}{\partial x} + v\frac{\partial v}{\partial y} + w\frac{\partial v}{\partial z} = \frac{1}{\mathrm{Re}}\Delta v - \frac{\partial p}{\partial y}, \tag{1.4}$$

$$\frac{\partial w}{\partial t} + u\frac{\partial w}{\partial x} + v\frac{\partial w}{\partial y} + w\frac{\partial w}{\partial z} = \frac{1}{\mathrm{Re}}\Delta w - \frac{\partial p}{\partial z}, \tag{1.5}$$

$$\frac{\partial u}{\partial x} + \frac{\partial v}{\partial y} + \frac{\partial w}{\partial z} = 0. \tag{1.6}$$

A *stationary solution* (laminar flow) $(\vec{u}_{ss}(x,y,z), p_{ss}(x,y,z))$ is a solution of the steady state Navier-Stokes equations

$$(\vec{u}_{ss} \cdot \nabla)\, \vec{u}_{ss} = -\nabla p_{ss} + \frac{1}{\mathrm{Re}} \Delta \vec{u}_{ss}, \tag{1.7}$$

$$\nabla \cdot \vec{u}_{ss} = 0. \tag{1.8}$$

We shall linearize the Navier-Stokes system (1.1)-(1.2) about this solution. To be precise, we consider stationary flow of the form $(\vec{u}_{ss}(x,y,z), p_{ss}(x,y,z)) = ((\bar{u}_{ss}(y), 0, 0)^T, p(x))$ and assume that the flow $\vec{u}$ is of the form

$$\vec{u}(t,x,y,z) = [\bar{u}_{ss}(y), 0, 0]^T + [\bar{u}(t,x,y,z), \bar{v}(t,x,y,z), \bar{w}(t,x,y,z)]^T$$

and the pressure has the form $p(t,x,y,z) = p_{ss}(x) + \bar{p}(t,x,y,z)$, where $\bar{u}$, $\bar{v}$, and $\bar{w}$ are small perturbations of the flow and $\bar{p}$ is a small perturbation of the pressure.

The resulting linearized Navier-Stokes equations which describe the flow field of perturbations $[\bar{u}(t,x,y,z), \bar{v}(t,x,y,z), \bar{w}(t,x,y,z)]^T$ near the "mean flow" $(\bar{u}_{ss}(y), 0, 0)^T$ are given

by

$$\frac{\partial \bar{u}}{\partial t} + \bar{u}_{ss}(y)\frac{\partial \bar{u}}{\partial x} + \bar{v}\frac{d}{dy}\bar{u}_{ss}(y) = \frac{1}{\mathrm{Re}}\Delta\bar{u} - \frac{\partial \bar{p}}{\partial x}, \tag{1.9}$$

$$\frac{\partial \bar{v}}{\partial t} + \bar{u}_{ss}(y)\frac{\partial \bar{v}}{\partial x} = \frac{1}{\mathrm{Re}}\Delta\bar{v} - \frac{\partial \bar{p}}{\partial y}, \tag{1.10}$$

$$\frac{\partial \bar{w}}{\partial t} + \bar{u}_{ss}(y)\frac{\partial \bar{w}}{\partial x} = \frac{1}{\mathrm{Re}}\Delta\bar{w} - \frac{\partial \bar{p}}{\partial z}, \tag{1.11}$$

$$\frac{\partial \bar{u}}{\partial x} + \frac{\partial \bar{v}}{\partial y} + \frac{\partial \bar{w}}{\partial z} = 0. \tag{1.12}$$

Observe that the linearized system (1.9)-(1.12) is defined by three convection diffusion equations (1.9)-(1.11) along with the divergence condition (1.12). For example, if $\bar{u}_{ss}(y) = 1-y^2$, then $\bar{u}_{ss}(y)$ is called the Poiseuille flow and this has been the starting point for a number of recent channel flow control papers (see [5], [33] [34], [37] and [39]).

At this point we refer the interested reader to the papers by Bamieh, Henningson, Högberg and Jovanovich as well as the recent dissertation by Hoepffner [32] where they construct various simplifications of the previous models in order to develop state space models. This example was presented only to illustrate how convection diffusion equations arise naturally from linearizations of realistic fluid flow problems. The 1D Burgers' equation provides a "simpler" model problem that often provides insight into computational issues and has been used to test computational algorithms. We briefly describe this equation and introduce the control input as a function on the boundary.

1.2 The Controlled Burgers' Equation

As noted above, the 1D Burgers' Equation

$$\frac{\partial w(t,x)}{\partial t} + w(t,x)\frac{\partial w(t,x)}{\partial x} = \frac{1}{\mathrm{Re}}\frac{\partial^2 w(t,x)}{\partial x^2} \quad t>0, \quad 0<x<1, \tag{1.13}$$

is often used as a model problem to test numerical algorithms for possible application to the Navier-Stokes system. Burgers' equation has also provided considerable insight into difficulties that come from control problems (see [3], [13], [15] and [18]). In particular, Burgers' equation with Neumann boundary control

$$w_x(t,0) = u_1(t), \quad w_x(t,1) = u_2(t) \tag{1.14}$$

leads to many non-standard computational problems. The papers [2] and [13] contain a summary of these problems along with references to relevant work.

If one defines $w(t,x)$ to be a constant $w(t,x) \equiv w_{ss}$, then w_{ss} is a steady state solution of equation (1.13) with zero Neumann boundary conditions (i.e. with $u_1(t) \equiv u_2(t) \equiv 0$). Therefore, the "linearization" of (1.13)-(1.14) about w_{ss} is given by

$$\frac{\partial \bar{w}(t,x)}{\partial t} + w_{ss}\frac{\partial \bar{w}(t,x)}{\partial x} = \frac{1}{\mathrm{Re}}\frac{\partial^2 \bar{w}(t,x)}{\partial x^2} \quad t>0, \quad 0<x<1,$$

where

$$\bar{w}_x(t,0) = u_1(t), \quad \bar{w}_x(t,1) = u_2(t).$$

This is a linear convection diffusion equation with Neumann boundary control.

1.3 A Convection Diffusion Control System

We close this chapter with a short review of how to set up a typical control system for the 1D convection diffusion equation. Motivated by the examples above, we consider the controlled convection diffusion equation

$$\frac{\partial w(t,x)}{\partial t} = \epsilon\frac{\partial^2 w(t,x)}{\partial x^2} - \kappa\frac{\partial w(t,x)}{\partial x} + b(x)u(t) \quad t>0, \quad 0<x<1, \tag{1.15}$$

with Dirichlèt boundary conditions

$$w(t,0) = 0, \quad w(t,1) = 0, \tag{1.16}$$

and initial condition

$$w(0,x) = w_0(x). \tag{1.17}$$

Here, $\epsilon > 0$, κ is constant and $b(\cdot) \in L^2(0,1)$ is a given function. The *control input* is the function $u(t)$. We assume that $\kappa > 0$. The case $\kappa < 0$ can be treated in an analogous fashion.

Define the convection diffusion operator, A_ϵ on $L^2(0,1)$ with domain

$$\mathcal{D}(A_\epsilon) = \left\{\varphi(\cdot) \in H^2(0,1) : \varphi(0) = 0, \quad \varphi(1) = 0\right\} \tag{1.18}$$

by

$$\left[A_\epsilon\varphi(\cdot)\right](x) = \epsilon\frac{d^2\varphi(x)}{dx^2} - \kappa\frac{d\varphi(x)}{dx}, \qquad \text{for all} \quad \varphi(\cdot) \in \mathcal{D}(A_\epsilon). \tag{1.19}$$

Note that for $\epsilon > 0$, $\mathcal{D}(A_\epsilon) = H_0^1(0,1) \cap H^2(0,1)$. For $\epsilon = 0$ it is natural to define

$$\mathcal{D}(A_0) = \left\{\varphi(\cdot) \in H^1(0,1) : \varphi(0) = 0\right\} \tag{1.20}$$

and

$$\left[A_0\varphi(\cdot)\right](x) = -\kappa\frac{d\varphi(x)}{dx}, \qquad \text{for all} \quad \varphi(\cdot) \in \mathcal{D}(A_0) \tag{1.21}$$

as a "limiting" operator as $\epsilon \to 0$. As noted in [48], often one can show that solutions of $A_\epsilon = f$ converge to $A_0 = f$, a result used to help design numerical schemes. This plays an important role in the analysis of convergence for the control problems considered later.

The Hilbert adjoint of A_ϵ, under the standard $L^2(0,1)$ inner product, is given by

$$\left[A_\epsilon^*\varphi(\cdot)\right](x) = \epsilon\frac{d^2\varphi(x)}{dx^2} + \kappa\frac{d\varphi(x)}{dx}, \qquad \text{for all} \quad \varphi(\cdot) \in \mathcal{D}(A_\epsilon^*) \tag{1.22}$$

where

$$\mathcal{D}(A_\epsilon^*) = \mathcal{D}(A_\epsilon) = \left\{\varphi(\cdot) \in H^2(0,1) : \epsilon\varphi(0) = 0, \quad \varphi(1) = 0\right\}. \tag{1.23}$$

Again we note that for $\epsilon > 0$, $\mathcal{D}(A_\epsilon^*) = H_0^1(0,1) \cap H^2(0,1)$. For $\epsilon = 0$, the Hilbert adjoint of A_0 given by (1.20)-(1.21) is defined on the domain

$$\mathcal{D}(A_0^*) = \left\{\varphi(\cdot) \in H^1(0,1) : \varphi(1) = 0\right\} \tag{1.24}$$

by

$$\left[A_0^*\varphi(\cdot)\right](x) = \kappa\frac{d\varphi(x)}{dx}, \qquad \text{for all} \quad \varphi(\cdot) \in \mathcal{D}(A_0^*). \tag{1.25}$$

Again we see that the representation of $\mathcal{D}(A_\epsilon^*)$ given by (1.23) suggests a natural limiting system.

Comment. The operator A_0 is highly non-normal. Thus, numerical methods for optimal feedback control problems need to take into account the issue of dual convergence. One needs to construct approximations of the operator A_0 that also approximate A_0^* (i.e., are stable and consistent to both). This can be a very difficult problem.

In order to complete the formulation of the control system, we define the linear operator $B : R^1 \to L^2(0,1)$ by

$$\left[Bu\right](x) = b(x)u$$

and note that B is a bounded linear operator with finite rank equal to one. If one defines the *state space* Z by $Z = L^2(0,1)$, then the controlled convection diffusion equation (1.15)-(1.17) is equivalent to the system

$$\dot{z}(t) = A_\epsilon z(t) + Bu(t), \qquad z(0) = z_0 \tag{1.26}$$

in $L^2(0,1)$.

1.4 The Spectrum and Numerical Ranges

For all $\epsilon \geq 0$, let A_ϵ be defined as above. If $\epsilon > 0$, straightforward calculations yield that the spectrum of A_ϵ consists only of the point spectrum given by real eigenvalues $\lambda_n(\epsilon)$, where for $n = 1, 2, 3, ...,$

$$\lambda_n(\epsilon) = -n^2\pi^2\epsilon - \frac{\kappa^2}{4\epsilon^2} = -(n^2\pi^2\epsilon + \frac{\kappa^2}{4\epsilon^2}). \tag{1.27}$$

Note that the largest eigenvalue is given by $\lambda_1(\epsilon) = -(\pi^2\epsilon + \frac{\kappa^2}{4\epsilon^2}) < 0$ and if λ is a complex number satisfying $\text{real}(\lambda) > \lambda_1(\epsilon) = -(\pi^2\epsilon + \frac{\kappa^2}{4\epsilon^2})$, then $\lambda \in \varrho(A_\epsilon)$ where $\varrho(A_\epsilon)$ is the resolvent set of A_ϵ. Also observe that the eigenvalues of the convection diffusion operator A_ϵ are the eigenvalues of the diffusion operator shifted to the left by $-\frac{\kappa^2}{4\epsilon^2}$. Since

$$\lambda_n(\epsilon) < \lambda_1(\epsilon) = -(\pi^2\epsilon + \frac{\kappa^2}{4\epsilon^2}) < -\frac{\kappa^2}{4\epsilon^2}$$

for all $n = 1, 2, 3, ...,$ it is clear that for each fixed $n \geq 1$, $\lambda_n(\epsilon) \to -\infty$ as $\epsilon \to 0$. Therefore, for $\epsilon < 1$, all eigenvalues of A_ϵ are bounded above by the fixed constant $-\frac{\kappa^2}{4}$. On the other hand, let $\varphi(\cdot) \in H_0^1(0,1) \cap H^2(0,1)$ be any function satisfying $\int_0^1 [\varphi(x)]^2\, dx = 1$ (say $\varphi(x) = \sqrt{2}\sin(\pi x)$), then

$$\langle A_\epsilon\varphi(\cdot), \varphi(\cdot)\rangle = -\frac{\epsilon}{2}$$

and the numerical range

$$NUM(A_\epsilon) \triangleq \{\langle A_\epsilon\varphi(\cdot), \varphi(\cdot)\rangle : \varphi(\cdot) \in \mathcal{D}(A_\epsilon), \quad \|\varphi(\cdot)\| = 1\}$$

is within $\frac{\epsilon}{2}$ of 0. The limiting operator A_0 has empty spectrum and the resolvent set $\varrho(A_0)$ is the entire complex plane. It is easy to show that the numerical range of A_0 is given by

$$NUM(A_0) = (-\infty, 0).$$

These simple observations play an important role in the understanding of some of the computational and convergence issues that arise in the feedback control problem.

We now review the standard linear Galerkin finite element approximation for the control system (1.26). The Galerkin finite element scheme is first order and sufficient for most applications. The stabilized Galerkin finite element method makes use of higher order terms and we shall use cubic elements to capture these terms. It is worthwhile to review the linear approximations so that one can see what additional terms are required in the stabilization process.

1.5 The Standard Linear Galerkin Finite Element Scheme

We review the basic methodology for constructing the standard linear finite element Galerkin approximation of the system (1.15)-(1.17). More details will be given later when we also derive the stabilized finite element scheme. The basic idea is to multiply both sides of the convection diffusion equation (1.15) by a "test function" $\psi(\cdot) \in H_0^1(0,1)$, integrate by parts and apply the boundary conditions (1.16) to yield the equation

$$\int_0^1 \frac{\partial w(t,x)}{\partial t}\psi(x)dx = -\epsilon \int_0^1 \frac{\partial w(t,x)}{\partial x}\psi'(x)dx - \kappa \int_0^1 \frac{\partial w(t,x)}{\partial x}\psi(x)dx + \left[\int_0^1 b(x)\psi(x)dx\right] u(t). \tag{1.28}$$

Thus, for all $\psi(\cdot) \in H_0^1(0,1)$, the variational equation (1.28) must hold and we say that $w(t,x)$ is a *weak solution* of (1.15)-(1.16) if (1.28) holds for all $\psi(\cdot) \in H_0^1(0,1)$ and $w(0,x) = w_0(x)$ almost everywhere on $(0,1)$.

If one defines the bilinear form $a_\epsilon(\cdot,\cdot)$ on $H_0^1(0,1) \times H_0^1(0,1)$ by

$$a_\epsilon(w(\cdot), v(\cdot)) = \int_0^1 \left[\epsilon \frac{dw(x)}{dx}\frac{dv(x)}{dx} + \kappa \frac{dw(x)}{dx}v(x)\right] dx, \tag{1.29}$$

for all $w(\cdot)$, $v(\cdot)$ in $H_0^1(0,1)$, then the variational equation (1.28) can be written as

$$\left\langle \frac{\partial w(t,\cdot)}{\partial t}, \psi(\cdot) \right\rangle_{L^2(0,1)} = -a_\epsilon(w(\cdot), \psi(\cdot)) + \left[\langle b(\cdot), \psi(x\cdot)\rangle_{L^2(0,1)}\right] u(t)$$

for all $\psi(\cdot) \in H_0^1(0,1)$.

The next step in approximating the system (1.26) is to choose a finite dimensional subspace of $H_0^1(0,1)$ and project onto this space. Let $x_i = \frac{i}{n+1}, \quad i = 0, 1, ..., n+1$ and define the piecewise linear, continuous splines $h_i^n(\cdot), \quad i = 1, ..., n$, on the interval $[0,1]$ by

$$h_i^n(x) = \begin{cases} \frac{1}{n}(x - x_{i-1}^n), & x \in [x_{i-1}^n, x_i^n], \\ \frac{1}{n}(x_{i+1}^n - x), & x \in [x_i^n, x_{i+1}^n], \\ 0 & \text{otherwise.} \end{cases} \tag{1.30}$$

The *finite element space* is the space $V_0^N \subset H_0^1(0,1)$ of dimension $N = n+1$, defined by

$$V_0^N \equiv \text{span}\{h_i^n(\cdot)\}_{i=1}^n.$$

If $a_\epsilon^N(\cdot,\cdot)$ is the bilinear form $a_\epsilon(\cdot,\cdot)$ restricted to the finite element space V_0^N, then $a_\epsilon^N(\cdot,\cdot)$ defines a bounded linear operator F_ϵ^N on V_1^n by

$$\left\langle \left[F_\epsilon^N w^N(\cdot)\right], v^N(\cdot)\right\rangle_{L^2(0,1)} = a_\epsilon^N(w^N(\cdot), v^N(\cdot)),$$

where $w^N(\cdot), v^N(\cdot) \in V_0^N$. Let $P^N : L^2(0,1) \to V_0^N$ be the orthogonal projection onto V_0^N and denote by $b^N(\cdot)$ and $w_0^N(\cdot)$ the orthogonal projection of $b(\cdot)$ and $w_0(\cdot)$ onto V_0^N, respectively. In particular, $b^N(\cdot) = P^N b(\cdot)$, $w_0^N(\cdot) = P^N w_0(\cdot)$. Finally, we define $G^N : \mathbb{R}^1 \to V_0^N$ by

$$\left[G^N u\right](x) = b^N(x)u.$$

The Galerkin finite element approximation to the system (1.26) is the finite dimensional system defined in V_0^N by

$$P^N\left[\frac{\partial}{\partial t}w(t,x)\right] = F_\epsilon^N w(t,x) + G^N u(t), \qquad P^N w(0,\cdot) = P^N w_0(\cdot) \in V_0^N. \tag{1.31}$$

If $P^N w(t,x) = w^N(t,x) = \sum_{i=1}^n z_i^n(t) h_i^n(x)$, then the system that defines the evolution of the coefficients $z^N(t) = [z_1^n(t), z_2^n(t), \ldots, z_n^n(t)]^T$ is given by the matrix equation

$$\mathbf{M}^N \dot{z}^N(t) = \mathbf{F}_\epsilon^N z^N(t) + \mathbf{G}^N u(t),$$

where $\mathbf{M}^N$ is the mass matrix, $\mathbf{F}_\epsilon^N$ is stiffness matrix and $\mathbf{G}^N$ is the control input matrix

defined by

$$\mathbf{G}^N = \begin{bmatrix} \mathbf{G}_1^N \\ \mathbf{G}_2^N \\ \vdots \\ \mathbf{G}_N^N \end{bmatrix},$$

where for $i = 1, 2, ..., n$,

$$\mathbf{G}_i^N = \langle b(\cdot), h_i^n(\cdot) \rangle_{L^2(0,1)}.$$

Clearly, the matrix representation of the approximate operators A_ϵ^N and B^N are given by

$$\mathbf{A}_\epsilon^N = \left[\mathbf{M}^N\right]^{-1} \mathbf{F}_\epsilon^N$$

and

$$\mathbf{B}^N = \left[\mathbf{M}^N\right]^{-1} \mathbf{G}^N,$$

respectively. Therefore, we have a Galerkin finite element approximation of the control system for the convection diffusion equation given by the finite dimensional system

$$\dot{z}^N(t) = \mathbf{A}_\epsilon^N z^N(t) + \mathbf{B}^N u(t). \tag{1.32}$$

The classical *simulation* problem is defined when the control function $u(t)$ and the initial data $w_0(x)$ are given and the finite element model (1.32) is integrated to generate the coefficients $z^N(t) = [z_1^n(t), z_2^n(t), ..., z_n^n(t)]^T$. This problem has a long history and is well understood. If the finite element matrices $\mathbf{A}_\epsilon^N$ and $\mathbf{B}^N$ are used to design a (feedback) controller, then additional convergence issues arise and require separate analysis depending on the particular design problem. For example, if one is attempting a linear quadratic regulator (LQR) design then Banks and Kunisch [7] have shown that the system $\left[\mathbf{A}_\epsilon^N, \mathbf{B}^N\right]$ must be stabilizable (uniformly in N).

If the system (1.32) is to be used for pole placement then $\left[\mathbf{A}_\epsilon^N, \mathbf{B}^N\right]$ must be controllable and it is possible to show (see [20]) that as $N \to +\infty$ the system $\left[\mathbf{A}_\epsilon^N, \mathbf{B}^N\right]$ approaches an uncontrollable system. Thus, one might expect that the use of (1.32) for pole placement will produce an ill-conditioned control problem. Although this area has been the subject of recent research efforts, many unanswered questions remain concerning convergence and conditioning of the approximating control problem. This is especially true for convection dominated problems and this is a main goal of the current thesis.

1.6 Notation and Overview

The following semigroup definitions are found in reference [45]. Define $L^2(\Omega)$, a Hilbert space, as the space of Lebesgue square integrable functions defined on Ω with the standard inner product

$$\langle \phi(\cdot), \psi(\cdot) \rangle_{L^2(\Omega)} = \int_\Omega \phi(x) \cdot \psi(x) d\Omega$$

We use standard notation for the Sobolev spaces $H^m(\Omega)$, where $H^m(\Omega)$ is the subspace of functions in $L^2(\Omega)$ whose partial derivatives up to order m are also in $L^2(\Omega)$ with norm

$$\|\phi(\cdot)\|_{H^m(\Omega)} = \sqrt{\sum_{i=0}^{m} \int_\Omega \left| \frac{\partial^i \phi(x)}{\partial x^i} \right|^2 \partial x}.$$

Likewise, $H_0^m(\Omega)$ is the completion of $C_0^\infty(\Omega)$ in $H^m(\Omega)$.

Let H be a Hilbert space with inner product $\langle \cdot, \cdot \rangle_H$. A one parameter family $T(t)$, $0 \leq t < \infty$, of bounded linear operators from $H \to H$ is a *semigroup of bounded linear operators* on H if

(i) $T(0) = I$, where I denotes the identity operator on H, and

(ii) $T(t+s) = T(t)T(s)$ for every $t, s \geq 0$.

A semigroup $T(t)$, $0 \leq t < \infty$, of bounded linear operators on the Hilbert space H is called *strongly continuous* if

$$\lim_{t \to 0^+} T(t)x = x \quad \text{for} \quad \text{every} \quad x \in H. \tag{1.33}$$

A strongly continuous semigroup is called a C_0-semigroup. We say that the linear operator A is the infinitesimal generator of the semigroup $T(t)$, if A is defined on the domain

$$\mathcal{D}(A) = \left\{ x \in X : \lim_{t \to 0^+} \frac{T(t)x - x}{t} \in H \quad \text{exists} \right\}$$

by

$$Ax = \lim_{t \to 0^+} \frac{T(t)x - x}{t}, \quad x \in \mathcal{D}(A).$$

An operator $A : D(A) \subset H \to H$ is called *dissipative* if

$$Re(\langle Ax, x \rangle_H) \leq 0, \quad \text{for} \quad \text{all} \quad x \in \mathcal{D}(A). \tag{1.34}$$

The operator A is said to be *maximally dissipative* if A is dissipative and there is no extension of A that remains dissipative. It can be shown that A is maximally dissipative if and only if both A and A^* are dissipative (see [45]).

A C_0-semigroup $T(t)$, $0 \leq t < \infty$ on H is *exponentially stable* if there exists constants $M \geq 1$ and $\omega > 0$ such that

$$\| T(t)x \|_X \leq Me^{-\omega t} \|x\|_H, \quad \text{for} \quad \text{all} \quad x \in H, \quad t \geq 0.$$

The following result may be found in [45] and is the basic result needed to establish that the operators defined by the convection diffusion operators generate well-posed problems.

Theorem 1 *Let H be a Hilbert space and assume A is a densely defined, closed linear operator on H. If both A and A^* are dissipative, then A is the infinitesimal generator of a C_0-semigroup of contractions on H. That is, if $S(t)$ is the C_0-semigroup generated by A, then $\|S(t)\|_{\mathcal{L}(H)} \leq 1$.*

We conclude this chapter with an overview of the main findings of the study.

1.7 Main Findings

This thesis is devoted to the problem of computing functional gains that define the optimal feedback LQR control laws for the convection diffusion equation (1.15)-(1.16). We concentrate on convection dominated problems defined to be those with Peclet number $Pe \triangleq \frac{|\kappa|}{\epsilon} >> 1$. The optimal feedback law has the form

$$u^{opt}(t) = -\int_0^1 \mathrm{K}(x)w(t,x)dx,$$

where $\mathrm{K}(\cdot) \in L^2(0,1)$ is called the functional gain. The problem with $\kappa = 0$ (i.e. the heat equation) has been studied in several papers and in this case standard finite element methods are usually well suited and lead to excellent numerical algorithms. The case where $Pe \triangleq \frac{|\kappa|}{\epsilon} >> 1$ had not received much attention until Vugrin's work [52]. We note that there is an excellent paper by Banks and Kunisch [8] that provides convergence proofs for the standard finite element method. However, the numerical results in [8] are restricted to

the diffusion dominated problem and as observed in [52] standard Galerkin finite elements tend to produce highly oscillatory approximations $\mathrm{K}^N(\cdot)$ of $\mathrm{K}(\cdot)$.

We conducted a careful numerical study of the impact that stabilization has on the convergence of the functional gains and the role that the stabilization parameter has on the convergence and accuracy. In general we discovered that:

1. The Galerkin Least Squares stabilized scheme can greatly improve both accuracy and rates of convergence if one is careful to select good stabilization parameters. The positive effect of stabilization is more important as the Peclet number becomes large.

2. On fine meshes both schemes approach the true functional gain and the errors produced by the stabilized schemes mostly occur in the "boundary layer" where the functional gain has a large gradient. This is very similar to what occurs in the simulation problem due to the fact that the numerical dissipation may be too large. The optimal stabilization parameter for simulation is not necessarily optimal for the Riccati equation.

3. All the numerical results imply that the functional gains computed by GLS method converge to the optimal gains. Indeed, even when the Peclet number is very large the stabilized gains converge and the error is dictated by the mesh size. This observation indicates that stabilization may provide a practical method for computing functional gains for complicated flow control problems such as the channel flow problem discussed above.

Chapter 2

Feedback Control of the Convection Diffusion Equation

We are concerned with the LQR control problem for linear convection-diffusion equations. We present numerical results for the one dimensional problem. Since the theoretical results are valid in any spatial dimension and the one dimensional problem is a special case, we formulate the problem in two dimensions in order to develop the mathematical framework for future research. Let $\Omega \subseteq \mathbb{R}^2$ be a bounded open domain with smooth boundary Γ. We consider the two dimensional convection diffusion equation with Dirichlèt boundary conditions given by

$$\frac{\partial}{\partial t}w(t,x,y) + \langle V, \nabla w(t,x,y)\rangle = \epsilon\nabla^2 w(t,x,y) + b(x,y)u(t), \tag{2.1}$$

$$w(t,x,y)|_\Gamma = g(x,y), \tag{2.2}$$

$$w(0,x,y) = w_0(x,y),$$

where $\epsilon > 0$ is the coefficient of thermal diffusivity and $V = [\ \kappa_1 \quad \kappa_2\ ]^T$ is the vector of convection coefficients. The function $b(x,y)$ is a given $1 \times m$ vector of the form $b(x,y) = [\ b_1(x,y),\ \ b_2(x,y),\ \ \cdots,\ \ b_m(x,y)\ ]$, where $b_i(x,y) \in L^2(\Omega)$ for $i = 1,2,...,m$. Here, $u(\cdot) = [\ u_1(\cdot),\ \ u_2(\cdot),\ \ \cdots,\ \ u_m(\cdot)\ ]^T \in L^2(0,+\infty;\mathbb{R}^m)$ is the control input function. We assume the initial data $w_0(\cdot,\cdot)$ belongs to $L^2(\Omega)$ and the boundary data $g(x,y)$ is sufficiently smooth so that equation (2.1) has a unique solution. In most cases, we limit our discussion to the homogeneous Dirichlèt boundary condition, $g(x,y) \equiv 0$.

Observe that equation (2.1) reduces to the standard heat equation when $V = 0$, and we say that equation (2.1) is convection dominated when $\epsilon << ||V||$. In this case, the convection term $\langle V, \nabla w(t,x,y)\rangle$ is significant and the uncontrolled equation (i.e., when $u(t) \equiv 0$) can have solutions with sharp gradients in small regions near the boundary. These regions are called boundary layers and lead to numerical difficulties if one does not take the special nature of the model into account. If one applies standard finite element and finite difference schemes to approximate equation 2.1, then very often the numerical results become highly oscillatory (see [25], [31], [46] and [48]).

Over the past twenty years considerable advances have been made in the development of special numerical methods to accurately simulate convection dominated flows. In the last section of this chapter we will briefly discuss and compare finite element schemes. Although we shall not attempt a complete review of all the work in this area, the interested reader can find excellent summaries in references [1], [23], [24], [25], [44] and [48]. We focus our study on so called stabilized finite element schemes. These schemes may be viewed as special upwind methods and remain a hot topic of investigation. Again, the interested reader might wish to look at a recent volume of the journal on "Computer Methods in Applied Mechanics and Engineering" (Volume 193, Issues 15 - 16, April 2004). This entire volume is devoted to recent advances on stabilized finite element methods. It is important to emphasize that all this work was concerned with the problem of *simulation* and until recently the idea of applying such stabilized methods to control problems had not been studied.

In order to motivate the research and to describe some of the potential computational issues, we present two simple examples that illustrate the basic points described above. The first example may be found in reference [48] and illustrates the idea of boundary layers.

Example 1. Consider the 1D boundary value problem given by

$$-\epsilon w''(x) + w'(x) = 1, \tag{2.3}$$

with boundary conditions

$$w(0) = 0, \qquad w(1) = 0. \tag{2.4}$$

This equation describes the steady state solution of the 1D version of the convection

diffusion equation (2.1) where $g(0) = g(1) \equiv 0$ and $u(t) \equiv 1$. Therefore, we would expect that as $t \to +\infty$ the solutions of equation (2.1) would converge to solutions of system (2.3)-(2.4). The exact solution to this boundary value problem is given by

$$w(x) = 1 - x - \frac{\exp(\frac{-x}{\epsilon}) - \exp(\frac{-1}{\epsilon})}{1 - \exp(\frac{-1}{\epsilon})},$$

and is plotted below.

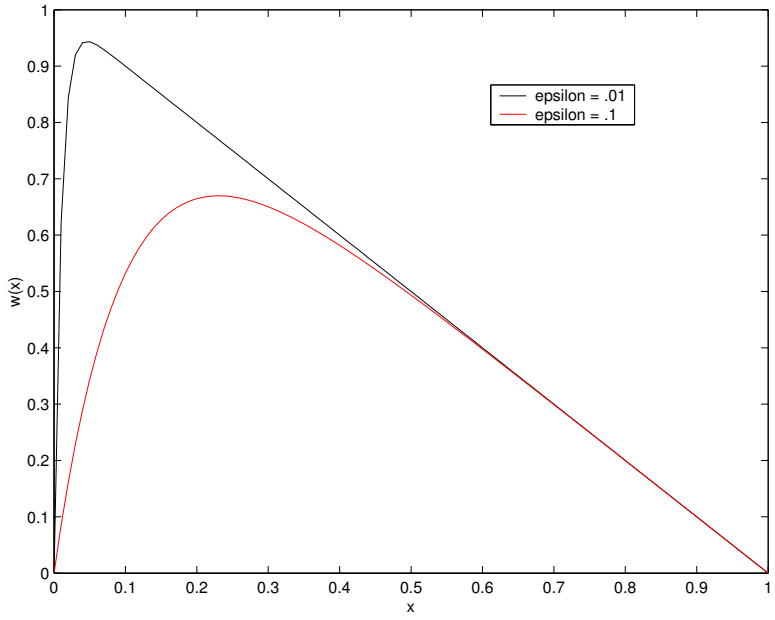

Figure 2.1: Solutions with Boundary Layers

Figure 2.1 contains plots of the exact solutions to the boundary value problem (2.3)-(2.4) for $\epsilon = 0.1$ and $\epsilon = 0.01$ respectively. Observe that for $\epsilon = 0.1$ the solution near $x = 0$ changes rapidly in the "boundary layer", roughly defined by the interval $(0, 0.2)$. In this region, the gradient $w'(x)$ is large when compared to the gradient on the remaining domain $(0.2, 1)$. Observe also that as epsilon decreases, the boundary layer becomes smaller. For $\epsilon = 0.01$, the boundary layer is now restricted to the interval $(0, 0.05)$. It is clear from this example that if one is constructing a numerical method to solve this boundary value problem for small ϵ, then a very fine grid might be required to resolve the equation near the boundary $x = 0$. Indeed, the next example will illustrate just one of several problems associated with the use of finite element methods to solve convection dominated problems.

Standard Galerkin finite element approximations correspond to centered finite difference schemes when the mesh is uniform. Such schemes do not take into account the direction of the "flow". For convection dominated problems, these methods often yield oscillatory solutions as can be seen in the following example taken from [25].

Example 2. Consider the 1D boundary value problem,

$$\kappa w'(x) - \epsilon w''(x) = 0, \tag{2.5}$$

on the interval $[0, 1]$ with $w(0) = 0$ and $w(1) = 1$. Again, this equation describes the steady state solution of the 1D version of the convection diffusion equation (2.1) where $g(0) = 0$, $g(1) = 1$ and $u(t) \equiv 0$. The exact solution on the interval $x = [0, 1]$ is given by

$$w(x) = \frac{\exp(\frac{\kappa x}{\epsilon}) - 1}{\exp(\frac{\kappa}{\epsilon}) - 1}, \tag{2.6}$$

and is plotted in Figure 2.2 where $\kappa = 2$ and $\epsilon = .1$.

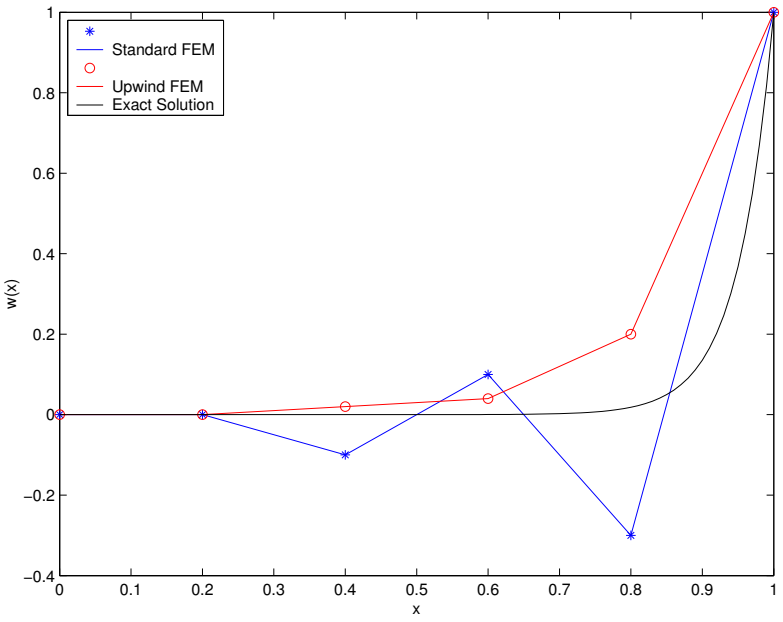

Figure 2.2: Oscillating Numerical Solutions

Notice that the boundary layer is located at the right end of the interval at $x = 1$. In this region the gradient $w'(x)$ is large when compared to the gradient on the remaining domain

$(0, .9)$. As stated previously, the solution in this boundary layer may be difficult to capture when using standard finite element approximations. Figure 2.2 illustrates typical solutions for various methods. Observe that the solution generated by standard piecewise linear finite elements produce numerical oscillations. As noted in [25], it is possible to reduce these oscillatory solutions by special numerical algorithms such as upwind and stabilized finite elements.

The previous examples illustrate some of the difficulties that motivated much of the development of upwind and stabilized finite element methods. We are concerned only with the application of these methods to control problems. In particular, we apply stabilization methods to the problem of computing functional gains for optimal feedback control. It is interesting to note that computational issues for control of the convection diffusion problem has not received much attention. As noted above, Vugrin's recent work [52] made use of transformation and re-norming methods. This thesis is concerned with the same class of problems. We focus on using stabilization techniques as a means to enhance convergence. In order to make these ideas precise, in the next section we briefly describe a typical control problem for the convection diffusion equation.

2.1 A Linear Quadratic Control Problem

We turn now to the formulation of a LQR control problem for the convection diffusion equation

$$\frac{\partial}{\partial t}w(t,x,y) + \langle V, \nabla w(t,x,y)\rangle = \epsilon\nabla^2 w(t,x,y) + b(x,y)u(t), \tag{2.7}$$

with Dirichlèt boundary conditions

$$w(t,x,y)|_\Gamma = 0, \tag{2.8}$$

initial condition

$$w(0,x,y) = w_0(x,y) \tag{2.9}$$

and distributed control. As above, $b(x,y)$ is a given $1 \times m$ vector of the form

$$b(x,y) = [\ b_1(x,y),\ \ b_2(x,y),\ \ \cdots, b_m(x,y)\ ],$$

$u(\cdot)$ is an $m \times 1$ vector function

$$u(\cdot) = [\ u_1(\cdot),\quad u_2(\cdot),\quad \cdots, u_m(\cdot)\ ]^T,$$

where $b_i(x,y) \in L^2(\Omega)$ and $u_i(\cdot) \in L^2(0,+\infty;\mathbb{R})$ for all $i = 1,2,...,m$. Also the initial data $w_0(\cdot,\cdot)$ belongs to $L^2(\Omega)$.

One can show that for $\epsilon > 0$, the uncontrolled problem (i.e., $u(t) \equiv 0$) is exponentially stable. However, when $0 < \epsilon << 1$ the decay rate is slow and convection dominates when $\epsilon << ||\,V||$. As noted above, in the 1D case, the numerical range is close to the imaginary axis and this implies that not only is the decay rate small, but also the system may become unstable for some small perturbations of the system. Therefore, one seeks a control law (feedback) that will improve the decay rate and enhance robustness. We concentrate on performance (i.e., the LQR problem), but most of the ideas apply to the Min-Max version of robust control theory (see [9], [17] and [22]).

The LQR optimal control problem provides one mechanism for computing a feedback control law that ensures stability of the closed-loop system and places "limits" on the control energy. In addition, this formulation can take advantage of spatial information in the formulation of the problem. In order to illustrate this feature we consider the 2D problem on a unit square $\Omega = (0,1) \times (0,1)$.

Assume that the goal of the control effort is to improve the rate of decay of the solution in a sub-domain $Q \subset \Omega$. Let $q(x,y)$ be defined on Ω by

$$q(x,y) = \begin{cases} q_u, & (x,y) \in Q \\ q_l, & (x,y) \notin Q \end{cases},$$

where $0 < q_l << q_u$. Observe that $0 < q_l \leq q(x,y) \in L^\infty(\Omega)$ and $q(x,y)$ is large on Q compared to the value on $\Omega - Q$. Let $R^T = R > 0$ be a real $m \times m$ symmetric positive definite matrix and define the LQR cost functional $J(u(\cdot))$ by

$$J(u(\cdot)) = \int_0^\infty \left[\int_\Omega q(x,y) w^2(t,x,y) dxdy + \langle Ru(t), u(t) \rangle_{\mathbb{R}^m} \right] dt, \tag{2.10}$$

where $w(t,x,y)$ is the solution to the system (2.7)-(2.9). The *LQR control problem* is defined by finding $u^{opt}(\cdot) \in L^2(0,+\infty;\mathbb{R}^m)$ such that

$$J(u^{opt}(\cdot)) \leq J(u(\cdot)) < +\infty$$

for all $u(\cdot) \in L^2(0, +\infty; \mathbb{R}^m)$.

Observe that this particular choice of $q(x, y)$ forces $w^2(t, x, y)$ to be small in the region Q and there is little penalty for large values of $w^2(t, x, y)$ on the complementary region $\Omega - Q$. One nice feature of first formulating the control problem in the PDE framework, is that this type of information can be used to help select the design parameters $q(x, y)$ and R.

In the next section we shall apply distributed parameter control theory to show the optimal LQR control exists and there is a function $\mathrm{K}(x, y) \in L^2(\Omega; \mathbb{R}^m)$ such that the optimal control has the representation

$$u^{opt}(t) = -\int_\Omega \mathrm{K}(x, y) w^{opt}(t, x, y) dxdy \tag{2.11}$$

The kernel $\mathrm{K}(x, y)$ is called the *functional gain* and has the form

$$\mathrm{K}(x, y) = [\ k_1(x, y), \quad k_2(x, y), \quad \cdots, \quad k_m(x, y)\ ]^T,$$

where each function $k_i(x, y) \in L^2(\Omega), i = 1, 2, 3, ..., m$. Actually, it is known that $k_i(x, y) \in H_0^1(\Omega)$ and this type of information is very useful in designing computational schemes (see [7]). The functional gain $\mathrm{K}(x, y)$ defines a bounded linear *feedback operator* $\mathcal{K} : L^2(\Omega) \to \mathbb{R}^m$ given by

$$\mathcal{K}\varphi(\cdot, \cdot) = \int_\Omega \mathrm{K}(x, y) \varphi(x, y) dxdy. \tag{2.12}$$

Observe that if one can compute the functional gain $\mathrm{K}(x, y)$, then the closed-loop system is given by the equation

$$\begin{aligned} \frac{\partial}{\partial t} w^{opt}(t, x, y) + \langle V, \nabla w^{opt}(t, x, y) \rangle &= \epsilon \nabla^2 w^{opt}(t, x, y) \\ &\quad - \int_\Omega \mathrm{K}(x, y) w^{opt}(t, x, y) dxdy, \end{aligned} \tag{2.13}$$

and is no longer a simple local (in space) partial differential equation. It is precisely this feature that makes the feedback law (2.11) so powerful. For example, this linear feedback law can have large impact on the non-linear system. This can be seen in [3], [15], [19] and [42] where such feedback controllers reduce the formation of shocks.

Another important feature of this representation has to do with the problem of sensor placement and the construction of practical reduced order dynamic controllers (see [14], [15],

[16], [17], and [19]). It follows from the representation (2.11) that for each $i = 1, 2, 3, ..., m$, the control $u_i^{opt}(t)$ is given by

$$\begin{aligned} u_i^{opt}(t) &= -\int_{\Omega} k_i(x,y) w^{opt}(t,x,y) dxdy \\ &= -\int_{SP(k_i(\cdot,\cdot))} k_i(x,y) w^{opt}(t,x,y) dxdy, \end{aligned}$$

where $SP(k_i(\cdot,\cdot))$ is the *support* of the function $k_i(\cdot,\cdot)$ given by

$$SP(k_i(\cdot,\cdot)) = \{(x,y) \in \Omega : k_i(x,y) \neq 0\}.$$

Therefore, the functional gain provides information about where in space to sense or where in space to construct estimators. The support of $k_i(\cdot,\cdot)$ provides valuable and practical information about the feedback law.

All of the above results depend on one being able to accurately compute the functional gain $\mathrm{K}(x,y)$. When the problem is convection dominated, the construction of accurate approximations to $\mathrm{K}(x,y)$ can be a difficult problem. Indeed, as observed by Vugrin in [52], standard finite element schemes that work very well for diffusion dominated problems fail to produce practical results for convection dominated problems. In this thesis we show that stabilized finite element schemes offer the potential for improved accuracy and faster convergence when compared to standard schemes. Here, we investigate the application of a GLS method to the problem of approximating the functional gain $\mathrm{K}(x,y)$.

In order to set the stage for the approximations, we now review the relevant distributed parameter LQR control theory and then formulate the PDE control problem as an abstract distributed parameter LQR problem. This formulation allows us to use the theory to obtain the representation (2.11) and provides a framework to construct numerical approximations to the functional gain $\mathrm{K}(x,y)$.

2.2 The Infinite Dimensional LQR Problem

In this section we summarize some basic results for the distributed parameter LQR problem. We use these results to provide a framework for constructing finite dimensional approximations to the functional gain $\mathrm{K}(x,y)$. Although the theory has a long history and is very

general, we concentrate only on the topics necessary to discuss the approximations. In particular, we use distributed control which means the control input operator is bounded.

We assume that the *state space* Z is a Hilbert space and the *control space* is also a Hilbert space U. Let $A : \mathcal{D}(A) \subset Z \to Z$ be the generator of a C_0-semigroup $S(t)$ on Z and assume that the *control input operator* is a bounded linear operator $B : U \to Z$. With this framework we consider the linear system in Z defined by

$$\dot{z}(t) = Az(t) + Bu(t), \tag{2.14}$$

with initial condition

$$z(0) = z_0 \in Z. \tag{2.15}$$

Given a control function $u(t)$ and initial condition z_0, the variation of parameters formula provides a representation of mild solutions given by

$$z(t) = S(t)z_0 + \int_0^t S(t-s)Bu(s)ds \tag{2.16}$$

and we use the word "solution" to mean "mild solution" defined by (2.16). Also, we need the following definition.

Definition The system (2.14) is said to be *stabilizable* if there exists a bounded linear operator $F : Z \to U$ such that the operator $A - BF$ is exponentially stable. In particular, (2.14) is stabilizable if the *closed-loop operator* $A - BF$ generates a C_0-semigroup $T(t)$ satisfying

$$\|T(t)\| \leq Me^{-\gamma t}$$

for some constants $M \geq 1$ and $\gamma > 0$.

Before we turn to the linear quadratic control problem, it is worth noting that such systems arise as linearizations of non-linear partial differential equations as briefly described by the channel flow problem in the previous chapter. If the operator A comes from a linearization about a non-trivial steady flow, the linear operator A is not normal and this can be the source of several difficulties. In addition, if one considers the resulting "small disturbance equation", then it has the form

$$\dot{z}(t) = Az(t) + F(z(t)) + Bu(t), \tag{2.17}$$

where A is not normal, $F(\cdot)$ is a non-linear function and is "conservative" in the sense that

$$\langle F(z), z\rangle = 0 \tag{2.18}$$

for all $z \in Z$ (see [6] and [13]). This structure, combined with robust control theory developed in the 1980s, is currently being applied to the age old problem of transition control. In order to provide a rigorous foundation for the analysis of the numerical algorithms used in the computation of these control laws, one must deal with the non-normality of the linear operator A and make a reasonable attempt to insure the conservative nature of the approximating non-linear terms are preserved.

The basic idea is to use the linearized system (2.14) to design a linear control and then apply this controller to the full non-linear system (2.17). This approach has proven to be successful in all types of distributed parameter systems and recently Henningson and his group have successfully used this method to control wall bounded fluid flows (see [32] and [33]). This method begins by solving a linear control problem for the system governed by the linearized partial differential equations and this requires that some approximation be introduced in the process.

Let Q and R be bounded self-adjoint operators defined on Z and U, respectively. In addition, we assume $Q : Z \to Z$ satisfies $Q = Q^* \geq 0$ (i.e., Q is positive semi-definite) and $R : U \to U$ satisfies $R = R^* > 0$ (i.e., R is positive definite). For each $u(\cdot) \in L^2([0,\infty); U)$ define the quadratic cost functional $J(u(\cdot))$ by

$$J(u(\cdot)) = \int_0^\infty [\langle Qz(t), z(t)\rangle_Z + \langle Ru(t), u(t)\rangle_U]dt, \tag{2.19}$$

where for $u(\cdot) \in L^2([0,\infty); U)$, $z(t)$ is the (mild) solution to (2.14)-(2.15) defined by (2.16). The LQR problem is to find $u^{opt}(\cdot) \in L^2([0,\infty); U)$ such that

$$J(u^{opt}(\cdot)) \leq J(u(\cdot)) < +\infty,$$

for all $u(\cdot) \in L^2([0,\infty); U)$.

The basic idea is to find a control to make the *weighted energy* $\int_0^\infty [\langle Qz(t), z(t)\rangle_Z]dt$ "small", while keeping the *control energy* $\int_0^\infty [\langle Ru(t), u(t)\rangle_U]dt$ within bounds. For the case where $Q = I$, the identity operator on Z, if the the cost is finite, i.e. if $J(u(\cdot)) < +\infty$,

then both the state $z(t)$ and the control $u(t)$ must decay exponentially to zero as $t \to +\infty$. In order to provide a basis for this, we cite some well known results on the abstract LQR problem. These results and proofs may be found in [9].

Theorem 2 *Assume that A generates a C_0-semigroup on H, and B is a bounded linear operator from U into H. If the pair (A, B) is stabilizable, then there exists a unique optimal pair $(u^{opt}(\cdot), z^{opt}(\cdot))$ for the LQR problem. Furthermore,*

$$u^{opt}(t) = -R^{-1}B^*\Pi z^{opt}(t), \quad 0 < t < \infty, \tag{2.20}$$

where Π is the self-adjoint, non-negative definite solution in $\mathcal{L}(H)$ of the Algebraic Riccati Equation (ARE)

$$\langle \Pi x, Ay\rangle_H + \langle \Pi Ax, y\rangle_H + \langle Qx, y\rangle_H - \langle R^{-1}B^*\Pi x, B^*\Pi y\rangle_U = 0 \tag{2.21}$$

for all $x, y \in \mathcal{D}(A)$. In addition, the optimal value of the cost is given by

$$J(u^{opt}(\cdot)) = \langle \Pi z_0, z_0\rangle_Z.$$

Observe that the representation (2.20) implies that

$$u^{opt}(t) = -Kz^{opt}(t), \quad 0 < t < \infty,$$

where $K : Z \to U$ is a *bounded* linear operator defined by

$$K = -R^{-1}B^*\Pi.$$

The operator K is called the *feedback gain operator* and the goal of this work is to compute K for the convection diffusion problem defined by (2.7)-(2.9) and a cost of the form (2.10). In order to make this statement precise we first formulate the partial differential equation (PDE) control problem as an abstract distributed parameter system (DPS) control problem.

2.3 The Abstract Formulation of the Convection Diffusion Control Problem

In order to formulate the PDE control problem (2.7)-(2.9) as an abstract LQR problem we begin as above and restrict our problem to the 2D problem on the unit square $\Omega =$

$(0,1) \times (0,1)$. Let $0 \leq q(x,y) \in L^\infty(\Omega)$ be given and recall that $b(x,y)$ is a given $1 \times m$ vector of the form $b(x,y) = [\ b_1(x,y),\ \ b_2(x,y),\ \ \cdots,\ \ b_m(x,y)\ ]$, where $b_i(x,y) \in L^2(\Omega)$ for all $i = 1, 2, ..., m$. Let $Z = L^2(\Omega)$, $U = \mathbb{R}^m$ and define the operators $Q : L^2(\Omega) \to L^2(\Omega)$ and $B : \mathbb{R}^m \to L^2(\Omega)$ by

$$[Q\varphi(\cdot,\cdot)](x,y) = q(x,y)\varphi(x,y)$$

and

$$[Bu](x,y) = b(x,y)u,$$

respectively.

Observe that since $q(x,y) \in L^\infty(\Omega)$ is essentially bounded, $Q : L^2(\Omega) \to L^2(\Omega)$ is a well defined bounded linear operator on $L^2(\Omega)$. Moreover, $Q = Q^*$ since

$$\begin{aligned}\langle Q\varphi(\cdot,\cdot), \psi(\cdot,\cdot)\rangle &= \int_\Omega [q(x,y)\varphi(x,y)]\psi(x,y)dxdy \\ &= \int_\Omega \varphi(x,y)[q(x,y)\psi(x,y)]dxdy \\ &= \langle \varphi(\cdot,\cdot), Q\psi(\cdot,\cdot)\rangle\end{aligned}$$

for all $\varphi(\cdot,\cdot)$ and $\psi(\cdot,\cdot)$ in $L^2(\Omega)$ and $0 \leq q(x,y)$ implies that

$$\langle Q\varphi(\cdot,\cdot), \varphi(\cdot,\cdot)\rangle = \int_\Omega q(x,y)[\varphi(x,y)]^2 dxdy \geq 0.$$

Therefore, $Q = Q^*$ is self-adjoint and positive semi-definite on $Z = L^2(\Omega)$.

If $u \in \mathbb{R}^m$, then

$$\|Bu\|_{L^2(\Omega)} = \sqrt{\int_\Omega \|b(x,y)u\|^2 dxdy} \leq \|b(\cdot,\cdot)\|_{L^2(\Omega)} \|u\|_{\mathbb{R}^m}$$

which implies that $B : \mathbb{R}^m \to L^2(\Omega)$ is a bounded linear operator. If $R = R^* > 0$ is an $m \times m$ positive definite matrix, then the cost function (2.10)

$$J(u(\cdot)) = \int_0^\infty \left[\int_\Omega q(x,y)w^2(t,x,y)dxdy + \langle Ru(t), u(t)\rangle_{\mathbb{R}^m}\right] dt$$

can be written as the cost function

$$J(u(\cdot)) = \int_0^\infty [\langle Qz(t), z(t)\rangle_Z + \langle Ru(t), u(t)\rangle_U]dt, \tag{2.22}$$

where $Z = L^2(\Omega)$ and $U = \mathbb{R}^m$.

In order to complete the formulation of the PDE control problem (2.7)-(2.9) we need to define the linear operator A. We use the standard formulation as suggested for the 1D problem in the previous chapter. Define A_ϵ on $\mathcal{D}(A_\epsilon) \subset L^2(\Omega)$ by

$$[A_\epsilon \varphi(\cdot,\cdot)](x,y) = \epsilon \nabla^2 \varphi(x,y) - \langle V, \nabla \varphi(x,y) \rangle \tag{2.23}$$

$$= \epsilon \nabla^2 \varphi(x,y) - \kappa_1 \frac{\partial}{\partial x}\varphi(x,y) - \kappa_2 \frac{\partial}{\partial y}\varphi(x,y), \tag{2.24}$$

where

$$\mathcal{D}(A_\epsilon) = H_0^1(0,1) \cap H^2(0,1). \tag{2.25}$$

The convection diffusion equation (2.7)-(2.9) becomes an abstract system on $Z = L^2(\Omega)$ defined by

$$\dot{z}(t) = A_\epsilon z(t) + Bu(t), \tag{2.26}$$

with initial data

$$z(0) = w_0 \in Z.$$

It is well known (see [7], [9], [43] and [45]) that A_ϵ generates a C_0-semigroup $S_\epsilon(t)$ on $Z = L^2(\Omega)$ and there exist constants $\alpha_\epsilon > 0$ and $M_\epsilon \geq 1$ such that

$$\|S_\epsilon(t)\| \leq M_\epsilon e^{-\alpha_\epsilon t} \tag{2.27}$$

for all $t \geq 0$. Actually, $S_\epsilon(t)$ is an analytic semi-group (see [7], [43] and [45]) and if $0 < \epsilon < \|V\| \neq 0$, then one can show that $\alpha_\epsilon \equiv \gamma > 0$ is a constant independent of ϵ. Therefore, if convection is present, then

$$\|S_\epsilon(t)\| \leq M_\epsilon e^{-\gamma t} \tag{2.28}$$

and the solutions to (2.26) decay uniformly in time. In general the coefficient $M_\epsilon \geq 1$ is not independent of ϵ and the case $M_\epsilon > 1$ can be the source of both theoretical and numerical difficulties.

The inequality (2.27) is sufficient to establish that the abstract convection diffusion control system (2.26) is stabilizable since the zero operator $F = \Theta : Z \to U$ meets the requirement in the definition of a stabilizable system. Therefore, we can apply the fundamental theorem from the previous section to obtain the following result.

Theorem 3 *There exists a unique optimal pair* $(u^{opt}(\cdot), z^{opt}(\cdot))$ *for the LQR problem defined by the convection diffusion equation (2.26) with cost (2.22). Furthermore,*

$$u^{opt}(t) = -\mathcal{K}_\epsilon z^{opt}(t), \quad 0 < t < \infty,$$

where K_ϵ *is given by*

$$\mathcal{K}_\epsilon = -R^{-1}B^*\Pi_\epsilon$$

and Π_ϵ *is the self-adjoint, non-negative definite solution of the Algebraic Riccati Equation*

$$A_\epsilon^*\Pi_\epsilon + \Pi_\epsilon A_\epsilon - \Pi_\epsilon B R^{-1} B^* \Pi_\epsilon + Q = 0. \tag{2.29}$$

If one applies the Riesz Representation theorem, then it follows that there exists a function

$$\mathrm{K}_\epsilon(x,y) = \left[\begin{array}{cccc} k_1(x,y), & k_2(x,y), & \cdots, & k_m(x,y) \end{array} \right]^T,$$

with $k_i(x,y) \in L^2(\Omega)$ for all $i = 1, 2, ..., m$, such that

$$\mathcal{K}_\epsilon \varphi(\cdot,\cdot) = \int_\Omega \mathrm{K}_\epsilon(x,y)\varphi(x,y)dxdy.$$

Thus, we have established the existence of the functional gain $\mathrm{K}_\epsilon(x,y)$ for the convection diffusion control problem. In addition, we now see that "computing" the feedback gain operator $\mathcal{K}_\epsilon$ is equivalent to approximating the functional gains $k_i(x,y) \in L^2(\Omega)$. We shall accomplish this by developing approximations of the Riccati equation (2.29).

Roughly speaking, we construct finite dimensional approximations A_ϵ^N, B^N and Q^N of A_ϵ, B and Q, respectively and solve an approximate Riccati equation

$$[A_\epsilon^N]^*\Pi_\epsilon^N + \Pi_\epsilon^N A_\epsilon^N - \Pi_\epsilon^N B^N R^{-1} [B^N]^* \Pi_\epsilon^N + Q^N = 0 \tag{2.30}$$

for Π_ϵ^N. The approximating functional gain is given by

$$\mathcal{K}_\epsilon^N = -R^{-1}[B^N]^*\Pi_\epsilon^N$$

and has the representation

$$\mathcal{K}_\epsilon^N \varphi(\cdot,\cdot) = \int_\Omega \mathrm{K}_\epsilon^N(x,y)\varphi(x,y)dxdy,$$

where

$$\mathrm{K}_{\epsilon}^{N}(x,y) = \left[\begin{array}{cccc} k_1^N(x,y), & k_2^N(x,y), & \cdots, & k_m^N(x,y) \end{array} \right]^T.$$

The important question is that of convergence. We are interested in numerical schemes (finite element and stabilized finite element) that lead to convergence of the functional gains in $L^2(\Omega)$. This issue is still the subject of current research. The general theory found in the Banks and Kunisch paper [8] places sufficient conditions on approximation schemes to guarantee the strong convergence of the gain operators. They showed that the standard conforming finite element scheme produces gain operators $\mathcal{K}_\epsilon$ such that

$$\lim_{N\to+\infty} \left\| \mathcal{K}_\epsilon^N \varphi(\cdot,\cdot) - \mathcal{K}_\epsilon \varphi(\cdot,\cdot) \right\|_{L^2(\Omega)} = 0$$

for all $\varphi(\cdot,\cdot) \in L^2(\Omega)$. Vugrin [52] has also established strong convergence of the functional gains in $L^2(\Omega)$. Thus, one has that for all $i = 1, 2, ..., m$,

$$\lim_{N\to+\infty} \left\| k_i^N(\cdot,\cdot) - k_i(\cdot,\cdot) \right\|_{L^2(\Omega)} = 0,$$

or more precisely,

$$\lim_{N\to+\infty} \sqrt{\int_\Omega \left| k_i^N(x,y) - k_i(x,y) \right|^2 dxdy} = 0.$$

The issue of how fast the functional gains converge, under mesh refinement, has not been settled. For convection dominated problems, convergence can be very slow if one applies a standard finite element scheme (see [52]). As $\epsilon \to 0$, the standard finite element scheme breaks down. One possible reason for this failure is that the approximating Riccati equation (2.30) seems to become ill-conditioned. We show that the stabilized GLS method enhances the rate of convergence and produces much better approximations on coarse grids.

Finally, we close this chapter with a comment about the general limiting problem. In the previous chapter we defined the 1D operator A_0 on the domain

$$\mathcal{D}(A_0) = H_L^1(0,1) \triangleq \left\{ \varphi(\cdot) \in H^1(0,1) : \varphi(0) = 0 \right\}$$

by

$$\left[A_0 \varphi(\cdot) \right](x) = -\kappa \frac{d\varphi(x)}{dx}, \qquad \text{for all} \quad \varphi(\cdot) \in \mathcal{D}(A_0)$$

as a "limiting" operator as $\epsilon \to 0$. There we assumed that $\kappa > 0$. This assumption was needed to ensure that the operator A_0 was the generator of a C_0-semigroup on $L^2(0,1)$. The

choice of an appropriate boundary condition is made by requiring that A_0 be dissipative. In particular, A_0 satisfies

$$\langle A_0\varphi(\cdot),\varphi(\cdot)\rangle_{L^2(0,1)} = \int_0^1 -\kappa\varphi'(x)\varphi(x)dx = -\frac{\kappa}{2}\varphi^2(x)\Big|_{x=0}^{x=1} = -\frac{\kappa}{2}\varphi^2(1) \leq 0,$$

for all $\varphi(\cdot) \in \mathcal{D}(A_0)$.

This approach extends to any dimension (see [46]) and provides a well-posed *dissipative* limiting dynamical system. The basic idea can be demonstrated by the 1D problem. Let $\Omega = (0,1)$ and note that the boundary of Ω is given by $\Gamma = \{0,1\}$. The outward normal to Ω at a point $x \in \Gamma$ is given by

$$\eta = \eta(x) = \begin{cases} +1, & x = 1 \\ -1, & x = 0 \end{cases}$$

and the *inflow boundary* Γ_- is defined by

$$\Gamma_- = \{x \in \Gamma : \eta(x)\kappa < 0\}.$$

If $\kappa > 0$, then it follows that the inflow boundary is $\Gamma_- = \{0\}$ and hence, the "correct" boundary condition for A_0 is the zero boundary condition on $\Gamma_- = \{0\}$. The selection of this boundary condition comes from the requirement that the "limiting operator" should generate a dynamical system and since all the operators A_ϵ are dissipative, the limiting operator should preserve this feature. Observe that each A_ϵ is dissipative in that for all $\varphi(\cdot) \in \mathcal{D}(A_\epsilon)$

$$\begin{aligned}\langle A_\epsilon\varphi(\cdot),\varphi(\cdot)\rangle_{L^2(0,1)} &= \epsilon\int_0^1 \frac{d^2}{dx^2}\varphi(x)\varphi(x)dx - \kappa_1\int_0^1 \frac{d}{dx}\varphi(x)\varphi(x)dx \\ &= \epsilon\frac{d}{dx}\varphi(x)\varphi(x)\Big|_{x=0}^{x=1} - \epsilon\int_0^1 [\frac{d}{dx}\varphi(x)]^2dx - \frac{\kappa}{2}[\varphi(x)]^2\Big|_{x=0}^{x=1} \\ &= -\epsilon\int_0^1 [\frac{d}{dx}\varphi(x)]^2dx \leq 0.\end{aligned}$$

Moreover, if A_ϵ is "lifted" to $\hat{A}_\epsilon : H^2(0,1) \to L^2(0,1)$, then for any $\varphi(\cdot) \in H^2(0,1)$

$$\left\langle \hat{A}_\epsilon\varphi(\cdot),\varphi(\cdot)\right\rangle_{L^2(0,1)} = \epsilon\frac{d}{dx}\varphi(x)\varphi(x)\Big|_{x=0}^{x=1} - \epsilon\int_0^1 [\frac{d}{dx}\varphi(x)]^2dx - \frac{\kappa}{2}[\varphi(x)]^2\Big|_{x=0}^{x=1}.$$

If we set $\epsilon = 0$, then

$$\begin{aligned}\left\langle \hat{A}_0\varphi(\cdot), \varphi(\cdot)\right\rangle_{L^2(0,1)} &= 0\left\{ \frac{d}{dx}\varphi(x)\varphi(x)\Big|_{x=0}^{x=1} - \int_0^1 [\frac{d}{dx}\varphi(x)]^2 dx \right\} - \frac{\kappa_1}{2}[\varphi(x)]^2\Big|_{x=0}^{x=1} \\ &= -\frac{\kappa}{2}[\varphi(1)]^2 + \frac{\kappa}{2}[\varphi(0)]^2.\end{aligned}$$

It follows that if $\kappa > 0$, then $\hat{A}_0$ will be dissipative if and only if $\varphi(0) = 0$ and if $\kappa < 0$, then $\hat{A}_0$ will be dissipative if and only if $\varphi(1) = 0$. Thus, we impose the Dirichlèt boundary condition on Γ_- where

$$\Gamma_- = \begin{cases} \{0\}, & \kappa > 0 \\ \{1\}, & \kappa < 0 \end{cases}.$$

When $\kappa > 0$, the boundary condition $\varphi(\cdot)|_{\Gamma_-} = 0$ makes A_0 a dissipative operator. However, the requirement that a restriction A_0 of $\hat{A}_0$ generate a C_0-semigroup on $L^2(0,1)$ forces A_0 to be maximally dissipative. This produces the correct domain $\mathcal{D}(A_0) = H_L^1(0,1) = \{\varphi(\cdot) \in H^1(0,1) : \varphi(0) = 0\}$.

Again, we emphasize that this idea extends to higher dimensions. It is important to formulate the limiting problem so that the corresponding limiting control problem is well-posed. The "correct" limiting boundary value problem defined by the convection equation depends on the choice of boundary conditions. This is important since many upwind and stabilized finite element schemes are motivated by the desire to capture the correct limiting dynamics (see [46] for details). We do not address this issue here, but we note that this aspect of these problems needs further study.

2.4 Approximations of the Convection Diffusion Equation

As was illustrated in Example 2, spurious oscillations develop when applying the standard finite element approximation schemes to the convection diffusion equation. To accurately compute a numerical solution to the convection diffusion equation, various finite element schemes have been developed over the years. These methods include (i) streamline upwind Petrov-Galerkin, (ii) stabilized least squares, (iii) explicit finite elements and (iv) upwind

triangle and secondary grid methods (see [48]). Streamline upwind Petrov-Galerkin (SUPG) is just one of many upwinding schemes that have been proposed. Pironneau (see [46]) discusses several of these methods, such as characteristics, upwinding by discretization of the total derivative, SUPG, and upwinding by discontinuity. We present a brief review of several stabilized finite element methods.

The SUPG method (see [12]) was first introduced by Brooks and Hughes in 1980. The SUPG method consists of adding to the weak form of the equation, a mesh dependent term that is pre-multiplied by a stability parameter. This term is a function of the Euler Lagrange equation. A modified weighting function is used to achieve the upwind effect. The element upstream of a node is weighted more heavily than the element downstream. This is applied to all terms of the equation thus resulting in a weighted residual formulation. The added term at the exact solution vanishes. In the context of the linear convection diffusion equation, SUPG performs better than the standard Galerkin finite element method (see [12], [24], [36]). However, spurious oscillations may remain when the exact solution has boundary layers [23].

The Galerkin Gradient Least Squares method discussed in reference [51] is typically employed when considering scalar second order partial differential equations that have second and zero order terms. The singular behavior emanates from a zero order term domination of the second order term. The perturbation that is added to the standard Galerkin form is developed using the gradient of the Euler Lagrange equation in a least squares formulation using linear elements.

The GLS formulation (see [26], [27], [28], [35], [41]) is the sum of the typical Galerkin finite element method and a weighted least squares formulation on each element. Mesh dependent terms that are functions of the Euler Lagrange equations evaluated element wise are added to the usual Galerkin method described above. Since the exact solution satisfies the residuals of the Euler Lagrange equations, consistency is preserved. Thus, stability is enhanced by these perturbation terms without destroying the consistency. The GLS method seems to be suitable for PDE's such as those governing structural problems.

More recently, the SUPG and the GLS methods have been used as a basis from which to develop new stabilized finite element methods. Another approach adds to the SUPG or GLS formulation, a term that attempts to capture the discontinuity. Namely, the Consistent

Approximate Upwind (CAU) method adds a non-linear term to the SUPG term, allowing for more regulation of the function's derivative in the direction of the gradient, eliminating the spurious oscillations (see [23], [24], [29]). The solution using CAU is much more stable than the GLS or SUPG methods. If the exact solution of the problem is smooth, then the CAU approximations creates crosswind diffusion, an undesirable effect (see [23], [29]). Effort has been directed to improving on the CAU method in reference [30].

While each of these methods have their benefits, the GLS approximation will be applied in the following chapters. In the realm of control design, GLS is easy to implement. We use this approximation for all numerical studies presented below.

Chapter 3

The Stabilized Galerkin Least Squares Method

In this chapter we develop the stabilized GLS approximation for the convection diffusion control problem. The approximation will be used to solve the Riccati equation that provides the feedback functional gains for the LQR problem. Although, the Riccati equation is time independent, we use the full time dependent residual to develop the approximating operators. In addition, as noted in [11] this approximation is best suited for simulating the convection dominated problem. We first review the standard Galerkin finite element approximation and then present the stabilized GLS scheme. Also, since the GLS scheme involves higher order spatial derivatives, we employ cubic splines in both methods.

3.1 The Standard Galerkin Finite Element Approximation

In this chapter we review a stabilized finite element method for the controlled 1D convection diffusion problem

$$\frac{\partial w(t,x)}{\partial t} = \epsilon \frac{\partial^2 w(t,x)}{\partial x^2} - \kappa \frac{\partial w(t,x)}{\partial x} + b(x)u(t) \quad t > 0, \quad 0 < x < 1, \tag{3.1}$$

with Dirichlèt boundary condition

$$w(t,0) = 0, \quad w(t,1) = 0. \tag{3.2}$$

The GLS approximation for the non-linear convection diffusion problem may be found in the references [3] and [42] where the derivation is similar to the approach in the papers [27] and [28]. It is well known that methods developed for steady state problems do not always provide stable numerical approximations for the time dependent problem (see [11]). One way to deal with this issue is to use the time dependent equation in the residual term when deriving the stabilization method. This is the approach taken in [3], [11], [27], [28], and [42]. We follow the general approach in [11] and specialize the presentation to the specific problem (3.1)-(3.2).

First, we need to recall the weak formulation of the system (3.1)-(3.2). Multiply both sides of (3.1) by a test function $\phi(\cdot)$ and integrate by parts to obtain

$$\begin{aligned}\int_0^1 w_t(t,x)\phi(x)dx &= \epsilon\int_0^1 w_{xx}(t,x)\phi(x)dx - \int_0^1 \kappa w_x(t,x)\phi(x)dx + \int_0^1 b(x)u(t)\phi(x)dx \\ &= \epsilon w_x(t,x)\phi(x)|_{x=0}^{x=1} - \epsilon\int_0^1 w_x(t,x)\phi'(x)dx \\ &\quad - \int_0^1 \kappa w_x(t,x)\phi(x)dx + \int_0^1 b(x)u(t)\phi(x)dx.\end{aligned}$$

We impose the geometric boundary conditions (3.2) on $w(t,x)$ and the test functions $\phi(\cdot)$. Thus, for all $\phi(\cdot) \in H_0^1(0,1)$, the above equation reduces to

$$\int_0^1 w_t(t,x)\phi(x)dx = \int_0^1 -\epsilon w_x(t,x)\phi'(x)dx - \int_0^1 \kappa w_x(t,x)\phi(x)dx + \int_0^1 b(x)u(t)\phi(x)dx, \tag{3.3}$$

and (3.3) defines the weak form of (3.1)-(3.2).

Observe that this is the form used to derive the standard finite element scheme outlined in the the first chapter. Recall that continuous piecewise linear splines given there are sufficient to produce a convergent scheme for the variational equation (3.3). The GLS stabilized scheme derived below contains higher order spatial derivatives and, although piecewise linear splines can be used in this case (see [3]), it requires that one "drop" the higher order derivatives. In order to recover these "lost" terms, King and Krueger [42] used cubic B-splines in the GLS approximation of the 1D Burgers' equation and could maintain all the stabilization terms. Before turning to the derivation of the GLS scheme, we review the cubic B-spline approximations.

Let $\{B_i(\cdot)\}_{i=-1}^{n+1}$ be the set of cubic B-splines on the interval $x = [0, 1]$ with n subintervals and $n+1$ uniformly spaced nodes, $0 = x_0 < x_1 < x_2 < \ldots < x_n = 1$. Let $dx = \frac{1}{n}$, then $B_i(\cdot)$ for $i = -1, 0, 1, 2, \ldots, n+1$ can be defined by

$$B_i(x) = \begin{cases} \frac{(x-x_{i-2})^3}{dx^3}, & x \in [x_{i-2}, x_{i-1}], \\ \frac{dx^3+3dx^2(x-x_{i-1})+3dx(x-x_{i-1})^2-3(x-x_{i-1})^3}{dx^3}, & x \in [x_{i-1}, x_i], \\ \frac{dx^3+3dx^2(x_{i+1}-x)+3dx(x_{i+1}-x)^2-3(x_{i+1}-x)^3}{dx^3}, & x \in [x_i, x_{i+1}], \\ \frac{(x_{i+2}-x)^3}{dx^3}, & x \in [x_{i+1}, x_{i+2}], \\ 0 & \text{elsewhere.} \end{cases}$$

The cubic B-splines that are used in the approximation of the 1D convection diffusion equation are represented in Figure 3.1.

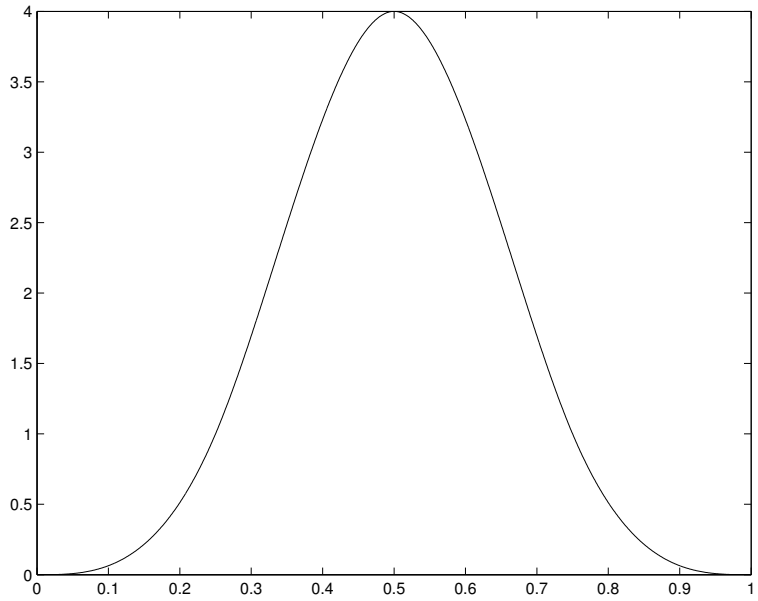

Figure 3.1: Cubic B-spline on [0,1]

When approximating (3.3) using finite elements, the Dirichlèt boundary conditions must be satisfied, thus we need a basis for a subspace that includes these boundary conditions. Observe that none of the functions $B_{-1}(\cdot)$, $B_0(\cdot)$, $B_1(\cdot)$, $B_{n-1}(\cdot)$, $B_n(\cdot)$, $B_{n+1}(\cdot)$ vanish at $x = 0$ and $x = 1$ so we need to eliminate these as possible basis functions. We define the

basis of cubic splines $\{\beta_i(\cdot) : i = 0, 1, ..., n\}$ by (see pages 208-209 in [47])

$$\beta_i^n(x) = \begin{cases} B_0(x) - 4B_{-1}(x), & i = 0, \\ B_0(x) - 4B_1(x), & i = 1, \\ B_n(x) - 4B_{n-1}(x), & i = n-1, \\ B_0(x) - 4B_{n+1}(x), & i = n, \\ B_i(x) & 2 \leq i \leq n-2. \end{cases}$$

It follows that

$$V_0^N = \text{span}\,\{\beta_i^n(\cdot) : i = 0, 1, ..., n\}$$

is an subspace of $H_0^1(0,1) \cap H^2(0,1)$ of dimension $N = n + 1$. The approximate "finite element approximation" is assumed to have the form $w(t,x) \approx w^N(t,x) = \sum_{i=0}^n w_i^n(t)\beta_i^n(x)$ and $w^N(t,x)$ is computed by solving a finite dimensional system of ordinary differential equations for the coefficients $w_i^n(t)$. This system is constructed by inserting the specific test functions $\phi(\cdot) = \beta_j^n(\cdot)$ into (3.3) for $j = 0, 1, 2, \ldots, n$ and writing the resulting equations as a matrix equation

$$\mathbf{M}^N \dot{w}^N(t) = -\epsilon \mathbf{A}_d^N w^N(t) - \kappa \mathbf{A}_c^N w^N(t) + \mathbf{B}_0^N u(t),$$

where

$$\mathbf{M}^N = \left[\int_0^1 \beta_i^n(x)\beta_j^n(x)dx\right]_{i,j=0}^n, \tag{3.4}$$

$$\mathbf{A}_d^N = \left[\int_0^1 [\beta_i^n(x)]' \left[\beta_j^n(x)\right]' dx\right]_{i,j=0}^n, \tag{3.5}$$

$$\mathbf{A}_c^N = \left[\int_0^1 [\beta_i^n(x)]' \left[\beta_j^n(x)\right] dx\right]_{i,j=0}^n, \tag{3.6}$$

$$\mathbf{B}_0^N = \left[\int_0^1 b(x)\beta_j^n(x)dx\right]_{j=0}^n \tag{3.7}$$

and

$$w^N(t) = \left[w_0^n(t), w_1^n(t), \ldots, w_n^n(t)\right]^T,$$

is the vector of coefficients.

Here, $\mathbf{M}^N$ is the mass matrix, $\mathbf{A}_d^N + \mathbf{A}_c^N$ is the stiffness matrix and $\mathbf{B}_0^N$ is the control input matrix. Note that for the remainder of this thesis, matrix representations with the

subscript d are associated with the diffusive term of the boundary value problem while matrices containing the subscript c are associated with the convection term. The standard form of this approximation to (3.3) can be written as

$$\begin{aligned}\dot{w}^N(t) &= -\epsilon[\mathbf{M}^N]^{-1}\mathbf{A}_d^N w^N(t) - \kappa[\mathbf{M}^N]^{-1}\mathbf{A}_c^N w^N(t) + [\mathbf{M}^N]^{-1}\mathbf{B}_0^N u(t) \\ &= \mathbf{A}^N w^N(t) + \mathbf{B}^N u(t), \\ w^N(0) &= w_0^N.\end{aligned} \tag{3.8}$$

When using this approximation in the following chapters of this thesis, it will be referred to as the unstabilized finite element approximation. We turn now to the derivation of the GLS approximation.

3.2 Galerkin Least Squares Approximation

Loosely speaking, the GLS approximation may be viewed as a perturbation of the standard (un-stabilized) Galerkin finite element system (3.8). One objective of the stabilization process is to produce approximations of the open-loop uncontrolled system that remain "numerically stable" for the case where $0 < \epsilon << \kappa$, i.e. for convection dominated problems. As we shall see later, numerical results in the following chapter imply that the same idea is of great benefit when stabilization is applied to the control problem. Although we proceed in the spirit of the paper [11], we present a continuum formulation of the GLS and use higher order elements in order to deal with the high order derivatives. We limit our discussion to the specific problem (3.1)-(3.2). The Galerkin method makes use of the weak form of (3.1)-(3.2) that is given by the variational equation

$$\int_0^1 w_t(t,x)\phi(x)dx = -\epsilon\int_0^1 w_x(t,x)\phi'(x)dx - \int_0^1 \kappa w_x(t,x)\phi(x)dx + \int_0^1 b(x)u(t)\phi(x)dx,$$

or equivalently,

$$\int_0^1 w_t(t,x)\phi(x)dx - \int_0^1 b(x)u(t)\phi(x)dx + G(w(t,\cdot),\phi(\cdot)) = 0, \tag{3.9}$$

where $G(w(\cdot),\phi(\cdot)) : H_0^1(0,1) \times H_0^1(0,1) \to \mathbb{R}^1$ is the standard (Galerkin) bilinear form defined by

$$G(w(\cdot),\phi(\cdot)) = \int_0^1 \epsilon w_x(t,x)\phi'(x)dx + \int_0^1 \kappa w_x(t,x)\phi(x)dx. \tag{3.10}$$

The time independent stabilization approach would replace $G(w(t,\cdot),\phi(\cdot))$ in (3.9) with a modified form

$$G_S(w(\cdot),\phi(\cdot)) \triangleq G(w(\cdot),\phi(\cdot)) + \langle R(w(\cdot)), W(\phi(\cdot))\rangle_{L^2(0,1)},$$

where $R(w(\cdot))$ is the residual of the steady problem (i.e., $u(t) \equiv u$) given by

$$R(w(x)) = \epsilon \frac{d^2w(x)}{dx^2} - \kappa \frac{dw(x)}{dx}$$

and $W(\phi(\cdot))$ is a *weighting operator*. There are several choices for the weighting operator and each choice produces a specific stabilization scheme. For the simple problem here, if

$$W_{SUPG}(\phi(x)) \triangleq \tau(x)\kappa\phi'(x),$$

where $\tau(\cdot)$ is a "*stability parameter*", then the resulting scheme is called the SUPG method. If

$$W_{GLS}(\phi(x)) \triangleq \tau(x)\left[-\epsilon\phi''(x) + \kappa\phi'(x),\right]$$

then one obtains the steady GLS method (see [11]).

In order to obtain an unsteady version of the GLS stabilization one replaces the residual with the full unsteady convection diffusion equation. In particular, let

$$R_{us}(w(t,x)) = w_t(t,x) - \epsilon w_{xx}(t,x) + \kappa w_x(t,x) - b(x)u(t)$$

and define $G_{GLS}(w(t,\cdot),\phi(\cdot))$ by

$$G_{GLS}(w(t,\cdot),\phi(\cdot)) = G(w(t,\cdot),\phi(\cdot)) + \langle R_{us}(w(t,\cdot)), W_{GLS}(\phi(\cdot))\rangle_{L^2(0,1)} \tag{3.11}$$

We replace the standard weak form (3.9)

$$\int_0^1 w_t(t,x)\phi(x)dx - \int_0^1 b(x)u(t)\phi(x)dx + G(w(t,\cdot),\phi(\cdot)) = 0$$

by the variational problem

$$\int_0^1 w_t(t,x)\phi(x)dx - \int_0^1 b(x)u(t)\phi(x)dx + G_{GLS}(w(t,\cdot),\phi(\cdot)) = 0$$

which can be written as

$$\langle w_t(t,\cdot),\phi(\cdot)\rangle - \langle b(\cdot)u(t),\phi(\cdot)\rangle + G_{GLS}(w(t,\cdot),\phi(\cdot)) = 0. \tag{3.12}$$

In order to complete the formulation, let

$$E_{STAB}(t) = \langle w_t(t,\cdot), \phi(\cdot)\rangle - \langle b(\cdot)u(t), \phi(\cdot)\rangle + G_{GLS}(w(t,\cdot), \phi(\cdot)).$$

Expand the stabilization term in (3.11) and simplify to yield

$$\begin{aligned}
\langle R_{us}(w(t,\cdot)), W_{GLS}(\phi(\cdot))\rangle &= \langle (w_t(t,\cdot) - \epsilon w_{xx}(t,\cdot) + \kappa w_x(t,\cdot) - b(\cdot)u(t)), W_{GLS}(\phi(\cdot))\rangle \\
&= \langle (w_t(t,\cdot) - b(\cdot)u(t)), W_{GLS}(\phi(\cdot))\rangle \\
&\qquad + \langle (-\epsilon w_{xx}(t,\cdot) + \kappa w_x(t,\cdot)), W_{GLS}(\phi(\cdot))\rangle \\
&= \langle (w_t(t,\cdot) - b(\cdot)u(t)), \tau(\cdot)\left[-\epsilon\phi''(\cdot) + \kappa\phi'(\cdot)\right]\rangle \\
&\qquad + \langle (-\epsilon w_{xx}(t,\cdot) + \kappa w_x(t,\cdot)), \tau(\cdot)\left[-\epsilon\phi''(\cdot) + \kappa\phi'(\cdot)\right]\rangle .
\end{aligned}$$

The first two terms involving $w_t(t,\cdot)$ and $b(\cdot)u(t)$ are grouped with the first two terms in (3.12) which produces

$$\begin{aligned}
E_{STAB}(t) = \langle w_t(t,\cdot) - b(\cdot)u(t), (\phi(\cdot) + \tau(\cdot)\left[-\epsilon\phi''(\cdot) + \kappa\phi'(\cdot)\right])\rangle + G(w(t,\cdot), \phi(\cdot)) \\
+ \langle (-\epsilon w_{xx}(t,\cdot) + \kappa w_x(t,\cdot)), \tau(\cdot)\left[-\epsilon\phi''(\cdot) + \kappa\phi'(\cdot)\right]\rangle .
\end{aligned}$$

Define the *augmented inertial form* $M_S(w_t(t,\cdot), \phi(\cdot))$ and the *spatially stabilized Galerkin form* $G_S(w(t,\cdot), \phi(\cdot))$ by

$$M_S(w_t(t,\cdot), \phi(\cdot)) = \langle w_t(t,\cdot), \phi(\cdot)\rangle + \langle w_t(t,\cdot), \tau(\cdot)\left[-\epsilon\phi''(\cdot) + \kappa\phi'(\cdot)\right]\rangle$$

and

$$\begin{aligned}
G_S(w(t,\cdot), \phi(\cdot)) &= G(w(t,\cdot), \phi(\cdot)) + \langle (-\epsilon w_{xx}(t,\cdot) + \kappa w_x(t,\cdot)), \tau(\cdot)\left[-\epsilon\phi''(\cdot) + \kappa\phi'(\cdot)\right]\rangle \\
&= \epsilon\int_0^1 w_x(t,x)\phi'(x)dx + \int_0^1 \kappa w_x(t,x)\phi(x)dx \\
&\qquad + \langle (-\epsilon w_{xx}(t,\cdot) + \kappa w_x(t,\cdot)), \tau(\cdot)\left[-\epsilon\phi''(\cdot) + \kappa\phi'(\cdot)\right]\rangle ,
\end{aligned}$$

respectively. Also, let the *stabilized control form* be defined by

$$B_S(b(\cdot)u(t), \phi(\cdot)) = \langle b(\cdot)u(t), \phi(\cdot)\rangle + \langle b(\cdot)u(t), \tau(\cdot)\left[-\epsilon\phi''(\cdot) + \kappa\phi'(\cdot)\right]\rangle .$$

The stabilized convection diffusion equation is now defined by the variational problem

$$M_S(w_t(t,\cdot), \phi(\cdot)) + G_S(w(t,\cdot), \phi(\cdot)) = B_S(b(\cdot)u(t), \phi(\cdot)) \tag{3.13}$$

and is well-defined for all $\phi(\cdot) \in H_0^1(0,1) \cap H^2(0,1)$. This form is equivalent to the semi-discrete variational problem on page 2304 in [11], where $\sigma = -1$ and the system is written at the element level. For the problem here

$$\begin{aligned}\langle w_t(t,\cdot), \phi(\cdot) + \tau(\cdot)\left[-\epsilon\phi''(\cdot) + \kappa\phi'(\cdot)\right]\rangle = -\epsilon\int_0^1 w_x(t,x)\phi'(x)dx - \int_0^1 \kappa w_x(t,x)\phi(x)dx \\ + \langle \epsilon w_{xx}(t,\cdot), \tau(\cdot)\left[-\epsilon\phi''(\cdot) + \kappa\phi'(\cdot)\right]\rangle \\ - \langle \kappa w_x(t,\cdot), \tau(\cdot)\left[-\epsilon\phi''(\cdot) + \kappa\phi'(\cdot)\right]\rangle \\ + \langle b(\cdot)u(t), \phi(\cdot)\rangle \\ + \langle b(\cdot)u(t), \tau(\cdot)\left[-\epsilon\phi''(\cdot) + \kappa\phi'(\cdot)\right]\rangle\end{aligned} \tag{3.14}$$

and the only remaining issue is the selection of the stabilization parameter $\tau(\cdot) > 0$.

As noted in [11], [27] and [28], the "optimal choice" is dependent on the local *Peclet number* and depends on the particular finite element mesh so that the *element Peclet number* is used to select good stabilization parameters. The Peclet number, Pe, measures the relative weights of convective and diffusive terms and for the 1D problem on a unit interval

$$Pe = |\kappa| / \epsilon.$$

When $Pe > 1$ the problem is convection dominated. Since this is the focus of this thesis, we assume that $Pe > 1$ and follow the development in [11], [27] and [28]. The element Peclet number is defined by

$$Pe^n = \frac{m_n |\kappa| h^n}{2\epsilon}, \tag{3.15}$$

where $h^n = h = 1/n$ is the mesh size and m is a constant. We assume that $Pe^n > 1$ so that the stabilization parameter in [27] is defined by

$$\tau(x) \equiv \tau^n \triangleq \frac{h^n}{2|\kappa|}. \tag{3.16}$$

Observe that $Pe > 1$ implies that

$$\tau^n = \frac{h^n}{2|\kappa|} = \frac{Pe^n}{Pe^n}\frac{h^n}{2|\kappa|} = \frac{1}{Pe^n}\frac{m|\kappa| h^n h^n}{4\epsilon|\kappa|} \leq \frac{m[h^n]^2}{4\epsilon} = \frac{mh^2}{4\epsilon}$$

and as suggested in [27] we set $m = 1/3$. This provides an optimal estimate for piecewise linear elements. We shall see later that for cubic elements this estimate is not optimal

and the bound defined by m depends on the elements and the problem to be solved (i.e., a steady simulation, an unsteady simulation or the Riccati equation associated with the control problem). For example, Bochev, Gunzburger and Shadid suggested that for the time dependent simulation problem described in [11], a good choice of $\tau(x)$ is

$$\tau(x) \equiv \tau^n \triangleq \frac{h^n}{\sqrt{15}\,|\kappa|}$$

since this choice maximizes phase accuracy for the pure convection problem defined by the operator A_0 defined above. We shall vary τ^n to illustrate the impact the choice of τ^n has on the convergence of the control designs. In any case, observe that $\tau(x) \equiv \tau^n$ is a constant that depends only on the mesh size. Thus, we can simplify the variational equation in (3.14).

The second two lines in (3.14) are given by

$$\langle \epsilon w_{xx}(t,\cdot), \tau(\cdot)\left[-\epsilon\phi''(\cdot) + \kappa\phi'(\cdot),\right]\rangle - \langle \kappa w_x(t,\cdot), \tau(\cdot)\left[-\epsilon\phi''(\cdot) + \kappa\phi'(\cdot)\right]\rangle$$

and may be regrouped as

$$\begin{aligned} &-\epsilon^2 \langle w_{xx}(t,\cdot), \tau(\cdot)\phi''(\cdot)\rangle + \kappa\epsilon \langle w_x(t,\cdot), \tau(\cdot)\phi''(\cdot)\rangle \\ &+ \kappa\epsilon \langle w_{xx}(t,\cdot), \tau(\cdot)\phi'(\cdot),\rangle - \kappa^2 \langle w_x(t,\cdot), \tau(\cdot)\phi'(\cdot)\rangle . \end{aligned} \tag{3.17}$$

Since $\tau(x) \equiv \tau^n$, it follows that

$$\begin{aligned} \kappa\epsilon \langle w_x(t,\cdot), \tau(\cdot)\phi''(\cdot)\rangle &= \kappa\epsilon \int_0^1 w_x(t,x)\tau(x)\phi''(x)dx \\ &= \kappa\epsilon\tau^n \int_0^1 w_x(t,x)\phi''(x)dx \\ &= \kappa\epsilon\tau^n w_x(t,\cdot)\phi'(\cdot)|_{x=0}^{x=1} - \kappa\epsilon\tau^n \int_0^1 w_{xx}(t,x)\phi'(x)dx. \end{aligned}$$

Consequently, (3.17) reduces to

$$-\epsilon^2\tau^n \langle w_{xx}(t,\cdot), \phi''(\cdot)\rangle + \kappa\epsilon\tau^n w_x(t,\cdot)\phi'(\cdot)|_{x=0}^{x=1} - \kappa^2\tau^n \langle w_x(t,\cdot), \phi'(\cdot)\rangle$$

and the stabilized variational equation has the form

$$\begin{aligned}\langle w_t(t,\cdot), \phi(\cdot) + \tau^n \left[-\epsilon\phi''(\cdot) + \kappa\phi'(\cdot),\right]\rangle = -\epsilon \int_0^1 w_x(t,x)\phi'(x)dx - \int_0^1 \kappa w_x(t,x)\phi(x)dx \\ - \tau^n\epsilon^2 \langle w_{xx}(t,\cdot), \phi''(\cdot)\rangle \\ + \kappa\epsilon\tau^n w_x(t,\cdot)\phi'(\cdot)|_{x=0}^{x=1} \\ - \tau^n\kappa^2 \langle w_x(t,\cdot), \phi'(\cdot)\rangle \\ + \langle b(\cdot)u(t), \phi(\cdot)\rangle \\ + \tau^n \langle b(\cdot)u(t), [-\epsilon\phi''(\cdot) + \kappa\phi'(\cdot)]\rangle .\end{aligned} \tag{3.18}$$

This is the form one needs to compute the finite element matrices for the GLS stabilized system.

We now approximate these additional terms using the finite element method with cubic B-splines. The matrix representation of the GLS formulation can be developed using the approximation of $w(t,x) \approx w^N(t,x) = \sum_{i=0}^{n+1} w_i^N(t)\beta_i^N(x)$ as before and letting ϕ range over the basis functions,

$$\begin{aligned}\mathbf{M}^N\dot{w}^N(t) + \mathbf{M}_s^N\dot{w}^N(t) = -\epsilon\mathbf{A}_d^N w^N(t) - \mathbf{A}_{d,s}^N w^N(t) - \kappa\mathbf{A}_c^N w^N(t) \\ + \mathbf{A}_{c,s}^N w^N(t) - \mathbf{B}_0^N u(t) - \mathbf{B}_s^N u(t)\end{aligned} \tag{3.19}$$

where

$$\mathbf{M}_s^N = \left[\epsilon \int_0^1 \tau^n \left[\beta_i^n(x)\right]' \left[\beta_j^n(x)\right]' dx\right]_{i,j=0}^n + \left[\kappa \int_0^1 \tau^n \left[\beta_i^n(x)\right] \left[\beta_j^n(x)\right]' dx\right]_{i,j=0}^n, \tag{3.20}$$

$$\mathbf{A}_{d,s}^N = \left[-\epsilon^2 \int_0^1 \tau^n \left[\beta_i^n(x)\right]'' \left[\beta_j^n(x)\right]'' dx\right]_{i,j=0}^n, \tag{3.21}$$

$$\mathbf{A}_{c,s}^N = \epsilon\kappa\tau^n \begin{bmatrix} \mathbf{A}_d^N(1,1) & \cdots & 0 \\ \vdots & 0 & \vdots \\ 0 & \cdots & \mathbf{A}_d^N(n,n) \end{bmatrix} + \left[-\kappa^2 \int_0^1 \tau^n \left[\beta_i^n(x)\right]' \left[\beta_j^n(x)\right]' dx\right]_{i,j=0}^n, \tag{3.22}$$

$$\mathbf{B}_s^N = \left[\int_0^1 \tau^n(-\epsilon b(x) \left[\beta_j^n(x)\right]'' + \kappa b(x) \left[\beta_j^n(x)\right]')dx\right]_{j=0}^n, \tag{3.23}$$

and the other matrices are as in (3.4)-(3.7). The resulting differential equation becomes

$$(\mathbf{M}^N + \mathbf{M}_s^N)\dot{w}^N(t) = (-\epsilon\mathbf{A}_d^N + \mathbf{A}_{d,s}^N)w^N(t) + (-\kappa\mathbf{A}_c^N + \mathbf{A}_{c,s}^N)w^N(t) + (\mathbf{B}_0^N + \mathbf{B}_s^N)u(t), \tag{3.24}$$

or equivalently,

$$\begin{aligned}\dot{w}^N(t) = (\mathbf{M}^N + \mathbf{M}_s^N)^{-1}\left[(-\epsilon\mathbf{A}_d^N + \mathbf{A}_{d,s}^N) + (-\kappa\mathbf{A}_c^N + \mathbf{A}_{c,s}^N)\right] w^N(t) \\ + (\mathbf{M}^N + \mathbf{M}_s^N)^{-1}(\mathbf{B}_0^N + \mathbf{B}_s^N)u(t).\end{aligned} \tag{3.25}$$

Thus, we have the first order approximating system given by

$$\dot{w}^N(t) = \mathbf{A}_s^N w^N(t) + \mathbf{B}_s^N u(t), \qquad w^N(0) = w_0^N.$$

This stabilized GLS approximation will be used to approximate the functional gains in the numerical runs that follow. We now present the results of our numerical experiments.

Chapter 4

Numerical Results

In this chapter we present the results of several numerical experiments for the control problem defined by the 1D convection diffusion problem

$$\frac{\partial w(t,x)}{\partial t} = \epsilon \frac{\partial^2 w(t,x)}{\partial x^2} - 1 \cdot \frac{\partial w(t,x)}{\partial x} + b(x)u(t) \quad t > 0, \quad 0 < x < 1, \tag{4.1}$$

with Dirichlèt boundary condition

$$w(t,0) = 0, \quad w(t,1) = 0. \tag{4.2}$$

Observe that we fix $\kappa = 1$ so that the Peclet number $Pe = \frac{1}{\epsilon} = \epsilon^{-1}$. Most of the numerical runs involve the case where $Pe = \epsilon^{-1} >> 1$. We assume only one control input and restrict our attention to the LQR problem defined by the cost

$$J(u(\cdot)) = \int_0^\infty \left[\int_0^1 w^2(t,x)dx] + R[u(t) \right]^2 dt, \tag{4.3}$$

where $R > 0$. This corresponds to the case where the control weighting function $g(x) \equiv 1$. Also, we fix the control weighting factor to be $R = 0.1$. The control input function is given by $b(x) = e^x$ and hence the control problem (4.1)-(4.2) with cost function (4.3) is completely defined by

$$b(x) = e^x, \qquad g(x) = 1, \qquad R = 0.1. \tag{4.4}$$

Recall that the LQR optimal control has the form

$$u^{opt}(t) = -\int_0^1 \mathrm{K}(x) w^{opt}(t,x)dx, \tag{4.5}$$

where $\mathrm{K}(\cdot) \in L^2(0,1)$ is the functional gain. We apply and compare the standard and stabilized GLS finite element methods to the problem of computing $\mathrm{K}(\cdot)$ for a convection dominated problem.

The approach is as described above. We use the two Galerkin finite element methods to construct approximations of the operator Riccati equation

$$A_\epsilon^* \Pi_\epsilon + \Pi_\epsilon A_\epsilon - \Pi_\epsilon B R^{-1} B^* \Pi_\epsilon + Q = 0, \tag{4.6}$$

where the operators in (4.6) are defined in Chapter 2. This step is accomplished by constructing finite dimensional approximations A_ϵ^N, B^N and Q^N of A_ϵ, B and Q, respectively and solving the approximating Riccati equation

$$[A_\epsilon^N]^* \Pi_\epsilon^N + \Pi_\epsilon^N A_\epsilon^N - \Pi_\epsilon^N B^N R^{-1} [B^N]^* \Pi_\epsilon^N + Q^N = 0 \tag{4.7}$$

for Π_ϵ^N. The approximating gain operator is given by

$$\mathcal{K}_\epsilon^N = -R^{-1}[B^N]^* \Pi_\epsilon^N$$

and has the representation

$$\mathcal{K}_\epsilon^N \varphi(\cdot) = \int_\Omega \mathrm{K}_\epsilon^N(x)\varphi(x)dx.$$

Therefore, we produce an approximating functional gain $\mathrm{K}_\epsilon^N(\cdot)$. The only issue is which method is better suited for computing of $\mathrm{K}_\epsilon^N(\cdot)$.

We denote the standard Galerkin finite element approximation by

$$\mathbf{A}_\epsilon^N = -\epsilon[\mathbf{M}^N]^{-1}\mathbf{A}_d^N - \kappa[\mathbf{M}^N]^{-1}\mathbf{A}_c^N, \tag{4.8}$$

$$\mathbf{B}^N = [\mathbf{M}^N]^{-1}\mathbf{B}_0^N, \tag{4.9}$$

$$\mathbf{Q}^N = [\mathbf{M}^N]^{-1}\mathbf{M}^N, \tag{4.10}$$

and the GLS approximation by

$$\mathbf{A}_{\epsilon,GLS}^N = (\mathbf{M}^N + \mathbf{M}_s^N)^{-1}\left[(-\epsilon\mathbf{A}_d^N + \mathbf{A}_{d,s}^N) + (-\kappa\mathbf{A}_c^N + \mathbf{A}_{c,s}^N)\right], \tag{4.11}$$

$$\mathbf{B}_{GLS}^N = (\mathbf{M}^N + \mathbf{M}_s^N)^{-1}(\mathbf{B}_0^N + \mathbf{B}_s^N), \tag{4.12}$$

$$\mathbf{Q}_{GLS}^N = [\mathbf{M}^N + \mathbf{M}_s^N]^{-1}(\mathbf{M}^N + \mathbf{M}_s^N), \tag{4.13}$$

respectively. All the matrices are given in Chapter 3. We emphasize again that the stabilized system depends on the choice of the stabilization parameter $\tau(\cdot)$ and that there is no "optimal parameter" defined for the problem associated with the Riccati equation. Indeed, even for the simulation problem there is no single way to select $\tau(\cdot)$ (see [11], [27] and [28]). Since we are using cubic elements on a uniform grid in 1D, we shall test various parameters of the form

$$\tau^n = \tau^n(m) = \frac{1}{m}\frac{h^n}{2} = \frac{1}{2mn}, \tag{4.14}$$

where $1 \leq m$.

Using this notation, we compute approximations

$$\mathrm{K}_\epsilon^N(\cdot) \approx \mathrm{K}_\epsilon(\cdot) \tag{4.15}$$

based on the standard Galerkin finite element approximations (4.8)-(4.10) and

$$\mathrm{K}_{\epsilon,GLS}^N(m,\cdot) \approx \mathrm{K}_\epsilon(\cdot) \tag{4.16}$$

based on the GLS approximations (4.11)-(4.13), respectively. Since we are using cubic B-splines as a basis, it follows that the approximation functional gains $\mathrm{K}_\epsilon^N(\cdot)$ and $\mathrm{K}_{\epsilon,GLS}^N(m,\cdot)$ have the representations

$$\mathrm{K}_\epsilon^N(x) = \sum_{i=0}^{n} \left[k_\epsilon^N\right]_i \beta_i^n(x)$$

and

$$\mathrm{K}_{\epsilon,GLS}^N(x) = \sum_{i=0}^{n} \left[k_{\epsilon,GLS}^N\right]_i \beta_i^n(x),$$

respectively.

As indicated in the previous chapter, Vugrin proved that the standard linear Galerkin finite element scheme implemented on a uniform mesh produced convergent functional gains (in $L^2(0,1)$) (see [52]). One has the following result.

Theorem 4 *If* $\mathrm{K}_\epsilon^N(\cdot)$ *is the functional gain computed by the linear Galerkin finite element scheme, then*

$$\lim_{N\to+\infty} \sqrt{\int_0^1 \left|\mathrm{K}_\epsilon^N(x) - \mathrm{K}_\epsilon(x)\right|^2 dx} = 0.$$

It is straightforward to modify this proof to the cubic B-splines and hence we have the following results for the approximation (4.8)-(4.10).

Theorem 5 *If* $\mathrm{K}_\epsilon^N(\cdot)$ *is the functional gain computed by the standard cubic Galerkin finite element scheme (4.8)-(4.10), then*

$$\lim_{N\to+\infty} \sqrt{\int_0^1 \left|\mathrm{K}_\epsilon^N(x) - \mathrm{K}_\epsilon(x)\right|^2 dx} = 0.$$

As we shall see below, this theoretical result is not as useful as one might think. The standard scheme can produce highly oscillatory functional gains $\mathrm{K}_\epsilon^N(\cdot)$ and the convergence can be extremely slow.

In general, the numerical results in this chapter show that the functional gains $\mathrm{K}_{\epsilon,GLS}^N(m,\cdot)$ obtained by applying the GLS approach produce reasonable approximations even for coarse grids. For low values of n one obtains better estimates of $\mathrm{K}_\epsilon(\cdot)$ than the oscillatory gains $\mathrm{K}_\epsilon^N(\cdot)$ produced by the standard unstabilized method. Also, we shall see that the choice of the stabilization parameter $\tau^n(m) = \frac{1}{2mn}$ can have a great effect on the convergence. Although we do not present a proof that the stabilized functional gains $\mathrm{K}_{\epsilon,GLS}^N(m,\cdot)$ converge to $\mathrm{K}_\epsilon(\cdot)$, the numerical results indicate that this is true. More will be said about this issue in the closing remarks. We turn now to the numerical experiments.

4.1 Numerical Experiments

In all the numerical experiments presented below, we use the cubic B-spline basis $\beta_i^n(\cdot)$ defined above so the finite element space is given by

$$V_0^N = \mathrm{span}\,\{\beta_i^n(x) : i = 0, 1, ..., n\}$$

defined in the previous chapter. Although we ran several problems with various control parameters, we present results only for the control parameters given by (4.4) above. We investigate the impact that stabilization has on the computation of the approximating functional gains $\mathrm{K}_{\epsilon,GLS}^N(m,\cdot)$. These results are typical of the other runs and provide the essential

information necessary to evaluate the impact of stabilization. The figures below contain plots of the approximating functional gains $\mathrm{K}_\epsilon^N(\cdot)$ computed by standard unstabilized Galerkin finite elements and the approximating functional gains $\mathrm{K}_{\epsilon,GLS}^N(m,\cdot)$ computed by the stabilized GLS method. We vary both the mesh size $h^n = 1/n$ and the parameter m in the stabilization parameter $\tau^n(m) = \frac{1}{2mn}$.

The tables contain relative L^2-errors defined by

$$L^2 \text{ error } = \frac{\sqrt{\int_0^1 \left|\mathrm{K}_\epsilon^n(x) - \mathrm{K}_\epsilon^{converged}(x)\right|^2 dx}}{\sqrt{\int_0^1 \left|\mathrm{K}_\epsilon^{converged}(x)\right|^2 dx}}$$

for the unstabilized scheme and

$$L^2 \text{ error } = \frac{\sqrt{\int_\Omega \left|\mathrm{K}_{\epsilon,GLS}^n(m,x) - \mathrm{K}_\epsilon^{converged}(x)\right|^2 dx}}{\sqrt{\int_0^1 \left|\mathrm{K}_\epsilon^{converged}(x)\right|^2 dx}}$$

for the stabilized GLS scheme, respectively. Here, $\mathrm{K}_\epsilon^{converged}(\cdot)$ is the "converged" functional gain on the finest mesh. For the cases with $\epsilon = .1$, $\epsilon = .01$, and $\epsilon = .001$ it was sufficient to take $n = 512$ to produce a "converged" gain so that $\mathrm{K}_\epsilon^{converged}(\cdot) = \mathrm{K}_\epsilon^{512}(\cdot)$. The case with $\epsilon = .0001$ required a mesh size of $n = 800$ and hence $\mathrm{K}_\epsilon^{converged}(\cdot) = \mathrm{K}_\epsilon^{800}(\cdot)$.

4.1.1 Numerical Experiment 1: $\epsilon = .1$

As stated previously, we are concerned with convection dominated problems. We set the stage by considering a simple scenario, when $\epsilon = .1$. In this case the Peclet number is $Pe = \frac{1}{\epsilon} = 10$ and we expect the diffusion term to be significant. The stabilization parameter is varied from $\tau^n(1) = \frac{1}{2n}$ to $\tau^n(64) = \frac{1}{128n}$ and, as seen in Table 4.1, most of the error in the stabilized GLS approximations is due to the additional numerical dissipation. Figure 4.1 contains the plots of the approximating functional gains for the case $m = 1$ and $n = 8$, 16, 32, 64, 128 and 256. Observe that convergence of the stabilized scheme (bottom figure) is slower than the unstabilized scheme (top figure). Figure 4.2 provides a comparison of $\mathrm{K}_{\epsilon}^{256}(\cdot)$ and $\mathrm{K}_{\epsilon,GLS}^{256}(1,\cdot)$ and Figure 4.3 shows the same comparison for $m = 64$. As expected, when the stabilization parameter $\tau^n(m)$ is reduced by increasing $m = 64$ the plots of $\mathrm{K}_{\epsilon}^{256}(\cdot)$ and $\mathrm{K}_{\epsilon,GLS}^{256}(64,\cdot)$ are nearly identical. As we see later, for large values of the Peclet number selecting a good stabilization parameter becomes more crucial.

	L^2-error in Functional Gains when $\epsilon = .1$		
	Unstabilized Gains	Stabilized Gains $m = 1$	Stabilized Gains $m = 64$
n=8	.1546	.4933	.1465
n=16	.0919	.3174	.0871
n=32	.0548	.1947	.0497
n=64	.0291	.1208	.0236
n=128	.0134	.0800	.0082
n=256	.0046	.0567	.0013

Table 4.1: L^2-error: Unstabilized and Stabilized Gains

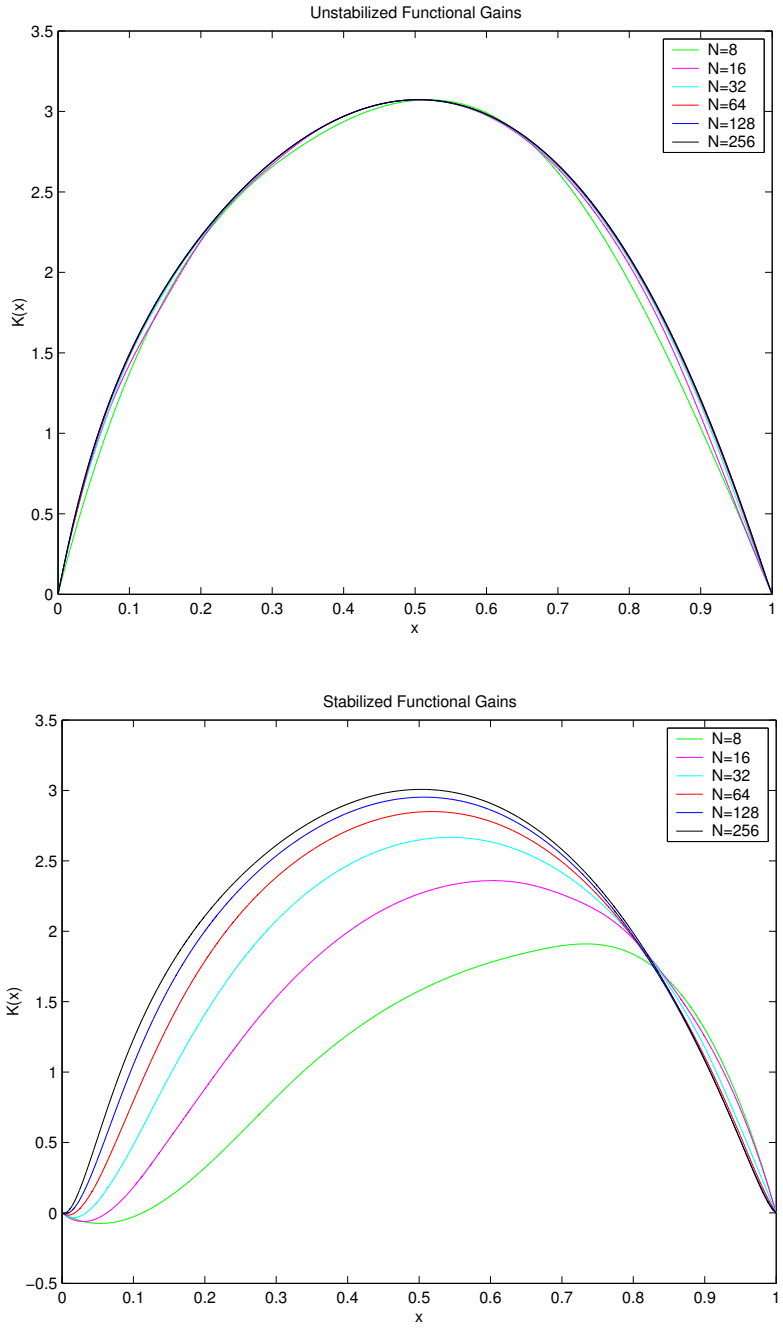

Figure 4.1: Epsilon = .1, m = 1: Unstabilized and Stabilized Gains

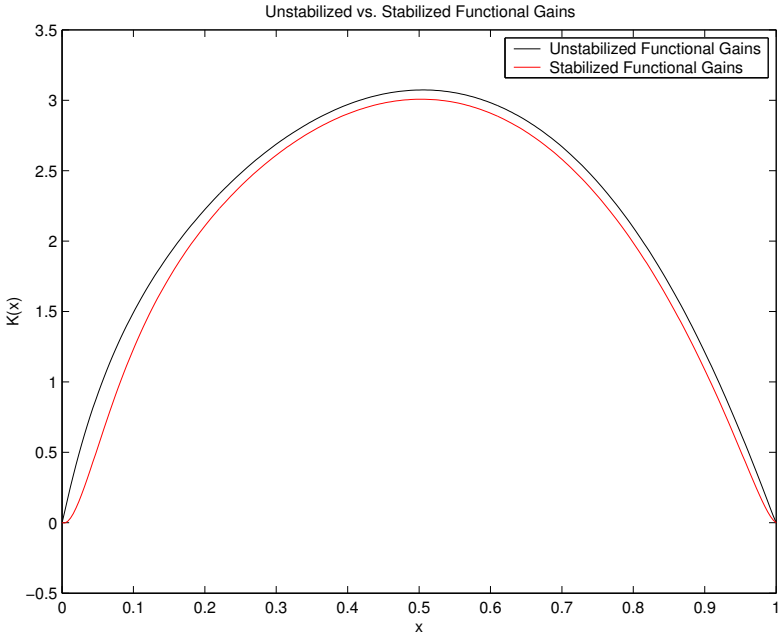

Figure 4.2: Epsilon = .1, m = 1: Unstabilized versus Stabilized Gains, n = 256

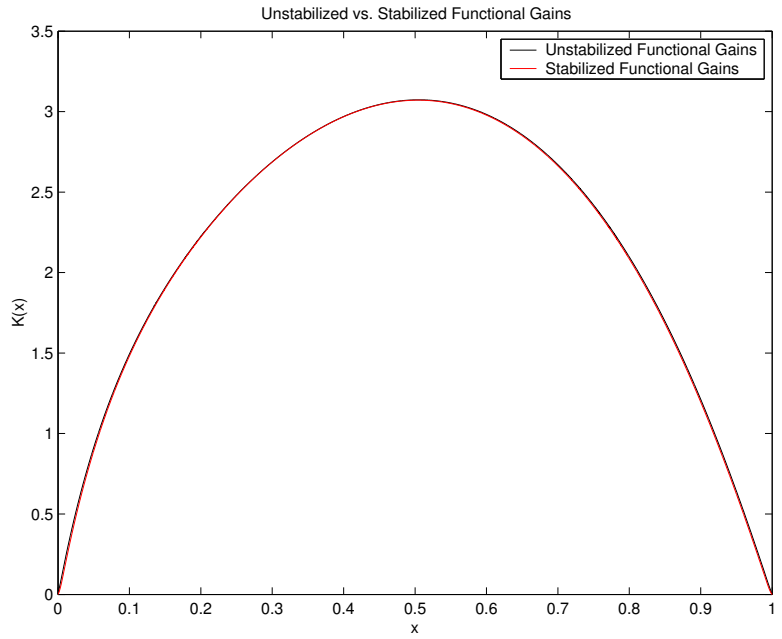

Figure 4.3: Epsilon = .1, m = 64: Unstabilized versus Stabilized Gains, n = 256.

4.1.2 Numerical Experiment 2: $\epsilon = .01$

For these runs, the diffusion parameter is decreased to $\epsilon = .01$ and hence the Peclet number is $Pe = \epsilon^{-1} = 100$. Therefore, convection is more important than in the previous experiment. We expect to see some difference in the functional gains computed by stabilized and unstabilized scheme. Thus, the choice of m should have more impact on the convergence of the stabilized functional gains. Figure 4.4 contains plots of the functional gains for both the unstabilized (top) and stabilized (bottom) scheme. As before we set $m = 1$ and $n = 8$, 16, 32, 64, 128, 256. Observe that for the coarse meshes (i.e., $n = 8$ and $n = 16$) both schemes produce oscillating gains, but as the mesh is refined both schemes smooth out and eventually converge. As illustrated in Figure 4.5 the stabilized functional gains retain a significant error and most of the error occurs in the "boundary layer" at $x = 0$. This error in the boundary layer is expected since the stabilization parameter introduces too much numerical dissipation. Decreasing $\tau^n(m)$ by setting $m = 4$ removes the oscillations on the coarse meshes. This is illustrated in Figure 4.6. As seen in Figure 4.7 the stabilized functional gains capture the correct boundary layer behavior. Finally, when $m = 8$ the stabilized functional gains have converged to the (correct) unstabilized functional gains. Figures 4.8 and 4.9 illustrate this convergence. We verify functional gain convergence by considering the L^2-error of the functional gains. Table 4.2 shows the error comparisons for the choices of m considered above.

	L^2-error in Functional Gains when $\epsilon = .01$			
	Unstabilized Gains	Stabilized Gains $m = 1$	Stabilized Gains $m = 4$	Stabilized Gains $m = 8$
n=8	.3676	.5469	.2039	.1673
n=16	.1365	.3039	.1264	.1000
n=32	.0589	.1952	.0842	.0604
n=64	.0294	.1297	.0500	.0323
n=128	.0136	.0844	.0273	.0154
n=256	.0048	.0527	.0151	.0072

Table 4.2: L^2-error: Unstabilized and Stabilized Gains

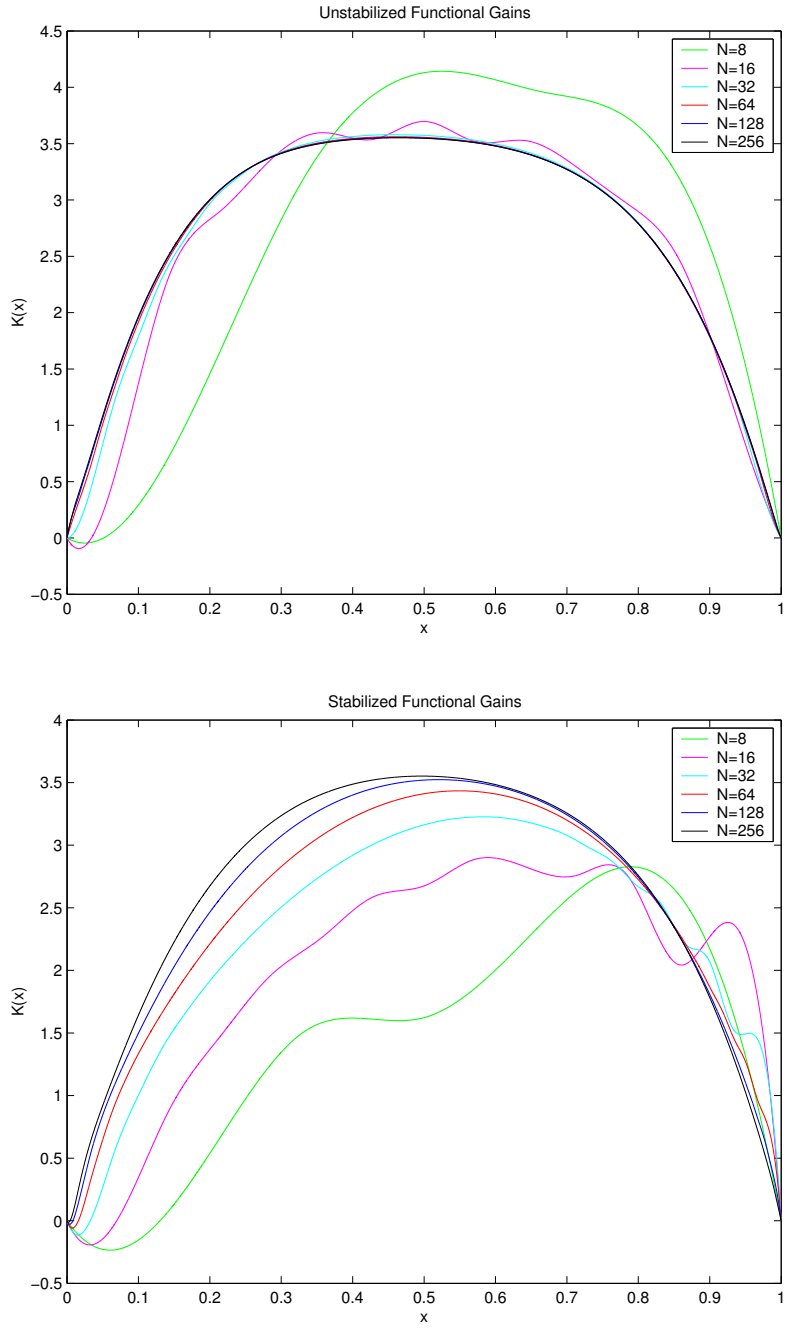

Figure 4.4: Epsilon = .01, m = 1: Unstabilized and Stabilized Gains

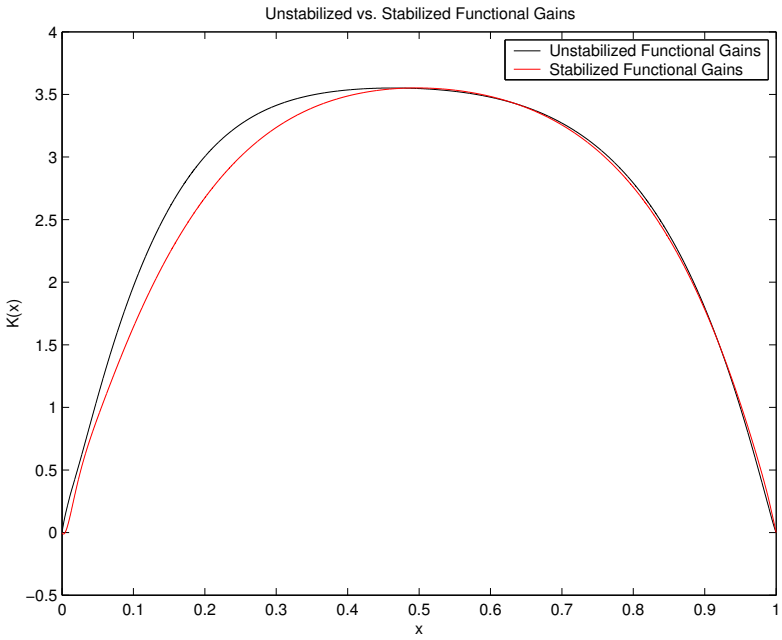

Figure 4.5: Epsilon = .01, m = 1: Unstabilized versus Stabilized Gains, n = 256

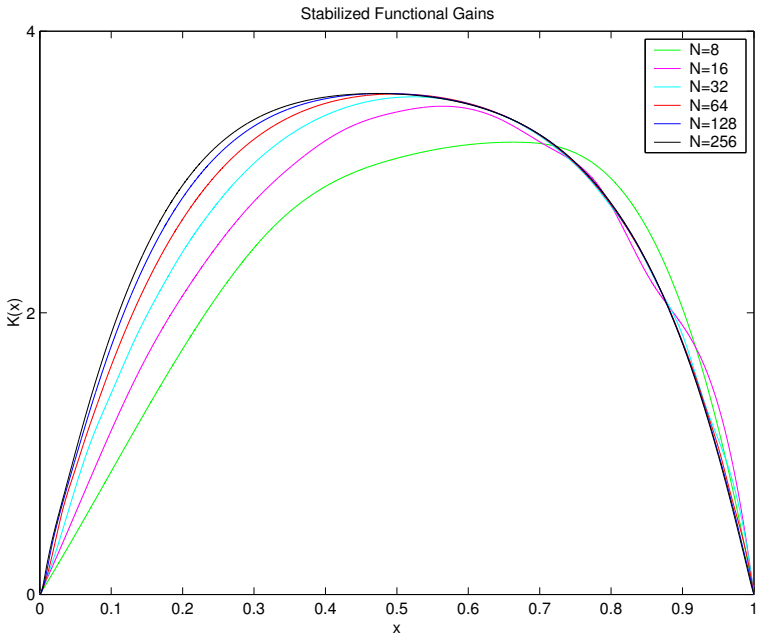

Figure 4.6: Epsilon = .01, m = 4: Stabilized Functional Gains

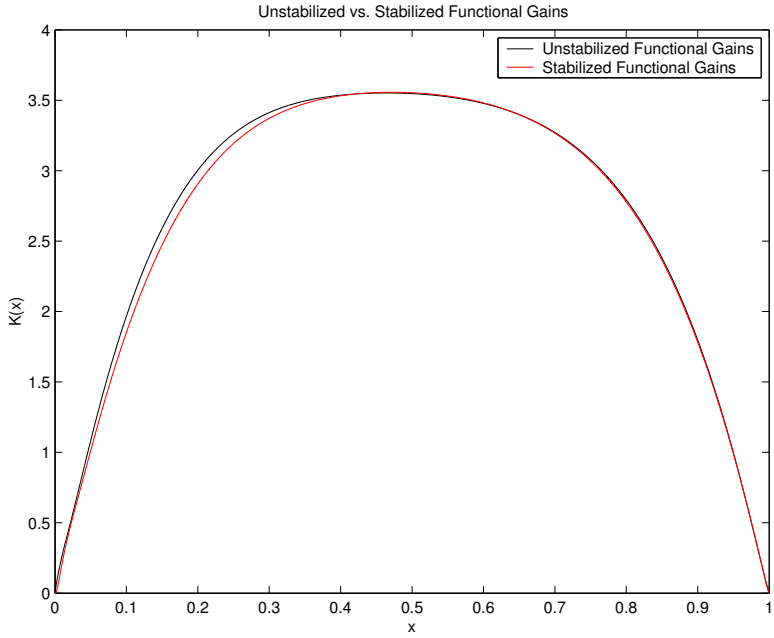

Figure 4.7: Epsilon = .01, m = 4: Unstabilized versus Stabilized Gains, n = 256

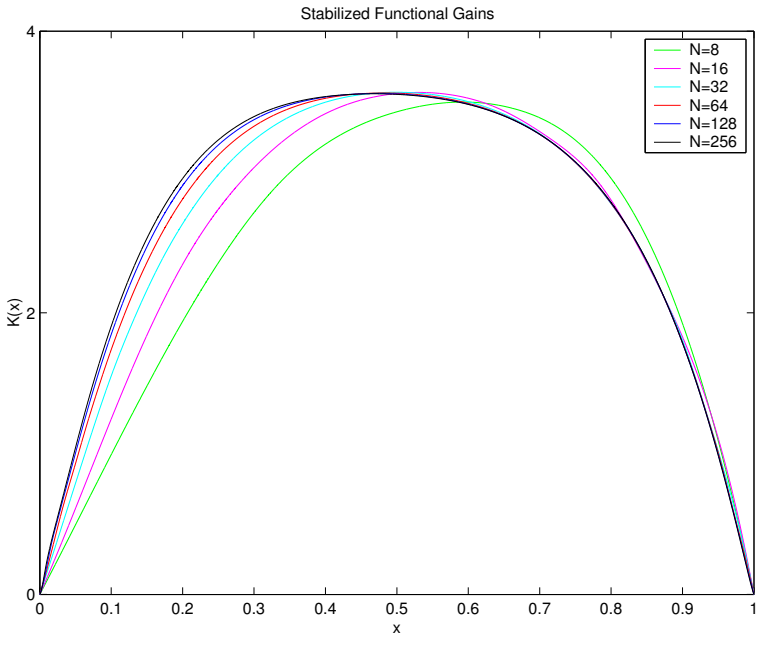

Figure 4.8: Epsilon = .01, m = 8: Stabilized Gains

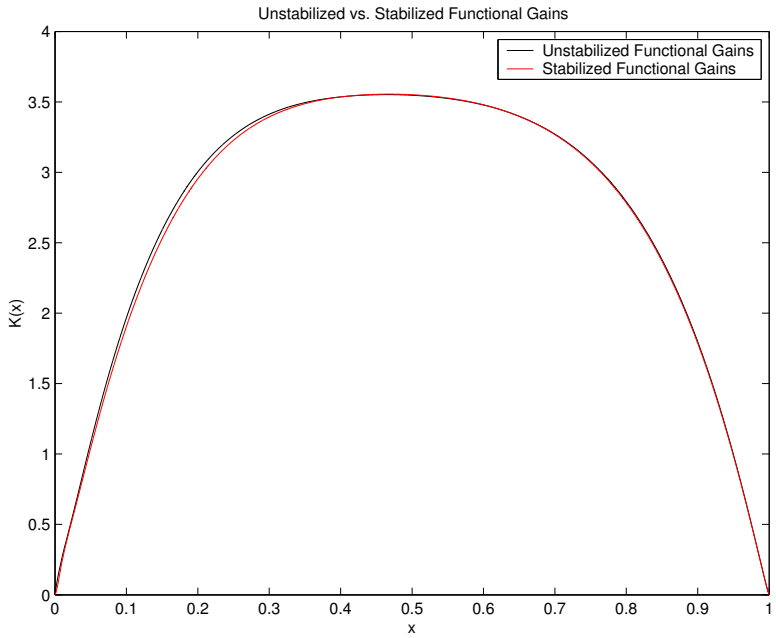

Figure 4.9: Epsilon = .01, m = 8: Unstabilized versus Stabilized Gains, n = 256

4.1.3 Numerical Experiment 3: $\epsilon = .001$

In this section we set $\epsilon = .001$ so that the Peclet number is $Pe = \epsilon^{-1} = 1000$. As observed in Figure 4.10 the unstabilized gains have large oscillations and these oscillations only diminish for very fine meshes. The oscillations are greatly reduced by stabilization if one sets $m = 4$. However, for $m = 4$ the additional numerical dissipation produces a significant error in the boundary layer as shown in Figure 4.11. If $\tau^n(m)$ is reduced by setting $m = 8$, then oscillations appear in the stabilized gains on coarse meshes as shown in Figure 4.12. However, these oscillations decay and essentially vanish for $n = 64$. Figure 4.13 compares the two gains for $m = 8$ and $n = 256$. Figures 4.14 and 4.15 show that by decreasing $\tau^n(m)$ to $\tau^n(16)$ the stabilized and unstabilized schemes both have oscillations on fine meshes. When one compares the oscillations for the stabilized gains in Figure 4.14 to the oscillations for the unstabilized scheme shown in Figure 4.10 one sees that stabilization greatly reduces the oscillations. Again, the relative L^2-errors are shown in Table 4.3.

	L^2-error in Functional Gains when $\epsilon = .001$			
	Unstabilized Gains	Stabilized Gains $m = 4$	Stabilized Gains $m = 8$	Stabilized Gains $m = 16$
n=8	2.0369	.3189	.2898	.2905
n=16	1.6221	.2223	.1849	.2138
n=32	.6644	.1814	.1435	.1520
n=64	.2053	.1439	.1057	.0904
n=128	.0588	.1067	.0713	.0493
n=256	.0154	.0731	.0445	.0257

Table 4.3: L^2-error: Unstabilized and Stabilized Gains

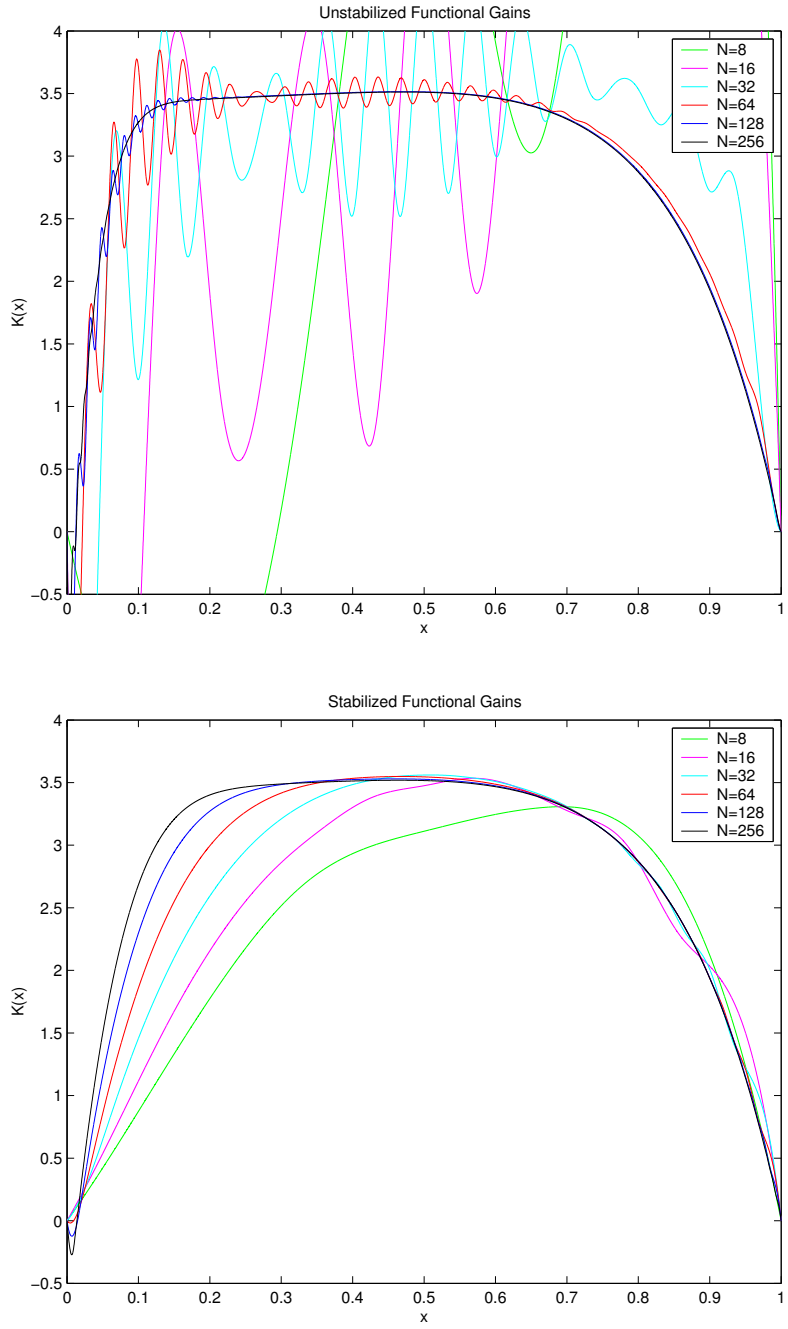

Figure 4.10: Epsilon = .001, m = 4: Unstabilized and Stabilized Gains

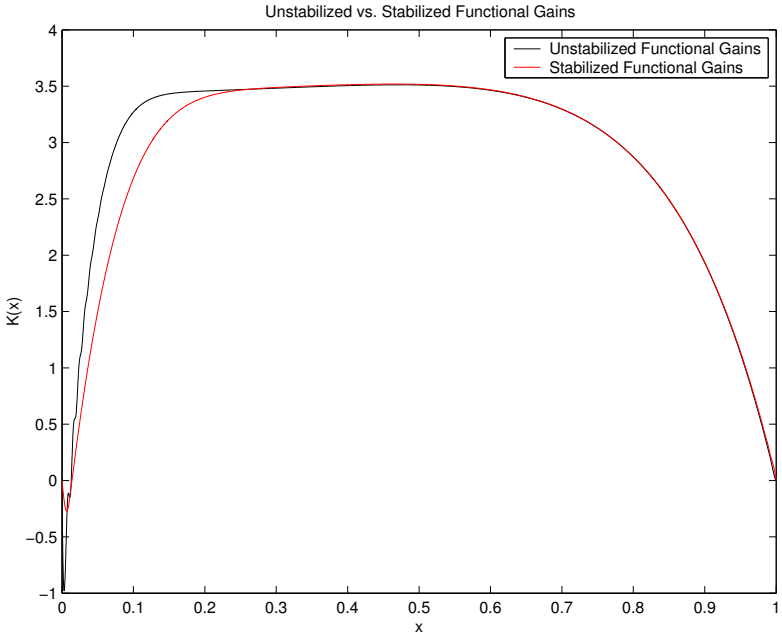

Figure 4.11: Epsilon = .001, m = 4: Unstabilized versus Stabilized Gains, n = 256.

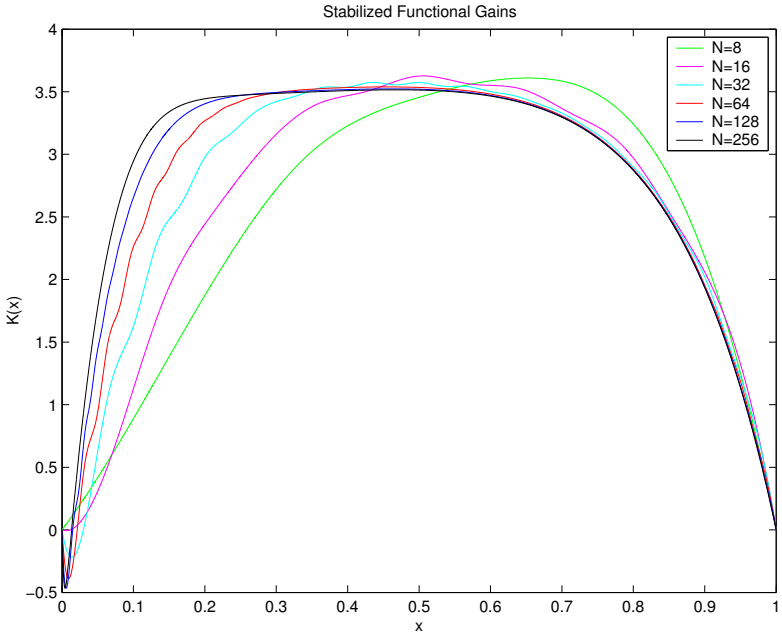

Figure 4.12: Epsilon = .001, m = 8: Stabilized Gains

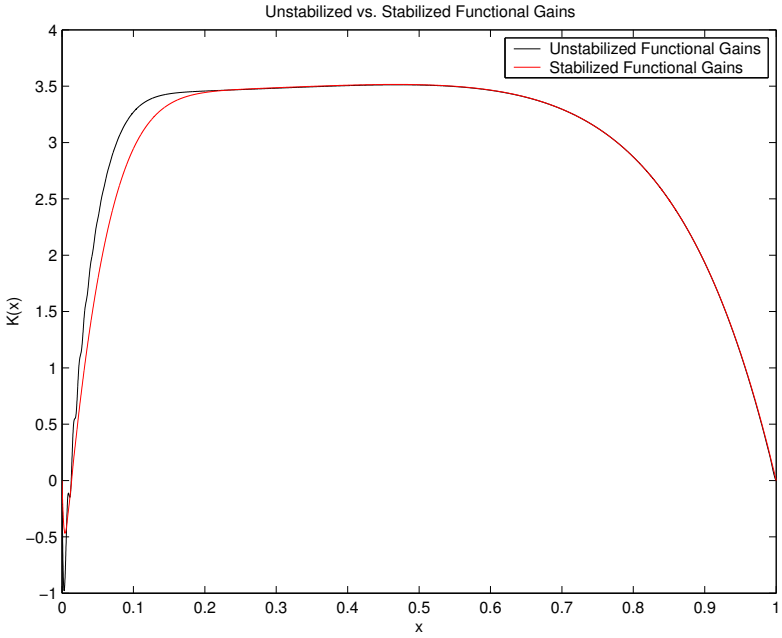

Figure 4.13: Epsilon = .001, m = 8: Unstabilized versus Stabilized Gains, n = 256.

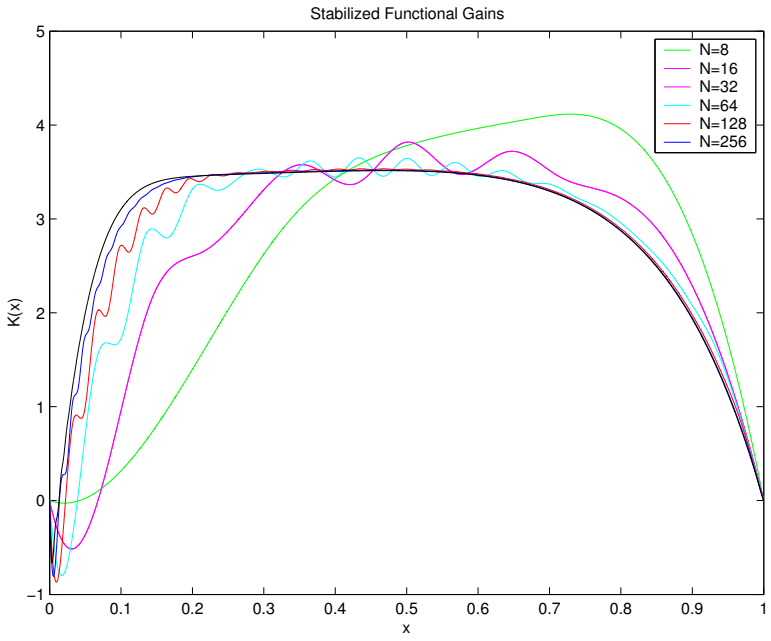

Figure 4.14: Epsilon = .001, m = 16: Stabilized Gains

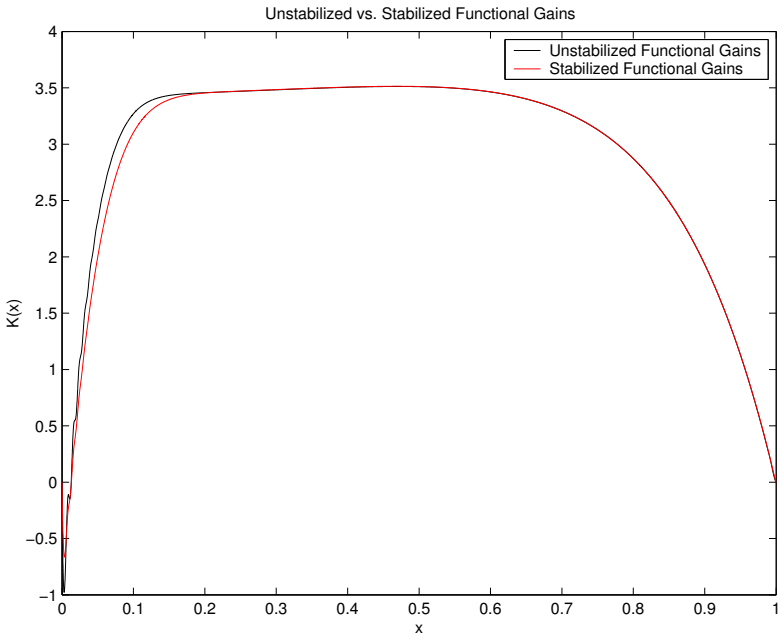

Figure 4.15: Epsilon = .001, m = 16: Unstabilized versus Stabilized Gains, n = 256

4.1.4 Numerical Experiment 4: $\epsilon = .0001$

In this set of experiments we set $\epsilon = .0001$ so that the Peclet number is $Pe = \epsilon^{-1} = 10,000$ and this represents a convection dominated problem. As illustrated in Figure 4.16, the unstabilized gains are oscillating even for small mesh sizes (e.g. when $n = 128$). For $m = 4$ the stabilized scheme produces only slight oscillations on the coarse meshes. Of course, as illustrated in Figure 4.17, the numerical dissipation yields greater error in the boundary layer. As m is increased from $m = 4$ to $m = 16$ we see the expected improvement in the boundary layer at the expense of oscillations appearing in the stabilized gains. This feature is clearly illustrated in the Figures 4.18, 4.19, 4.20 and 4.21. It is important to note that even with the slight oscillations produced by reducing $\tau^n(m)$, as shown in Table 4.4, the L^2-error is smaller for the stabilized gains.

	L^2-error $\epsilon = .0001$			
	Unstabilized Gains	Stabilized Gains $M = 4$	Stabilized Gains $M = 8$	Stabilized Gains $M = 16$
n=8	3.4750	.3746	.3500	.3415
n=16	3.8118	.2808	.2421	.2679
n=32	3.3550	.2412	.2004	.2229
n=64	1.8823	.2111	.1743	.1777
n=128	.6410	.1809	.1457	.1324
n=256	.2107	.1486	.1142	.0906

Table 4.4: L^2-error: Unstabilized and Stabilized Gains

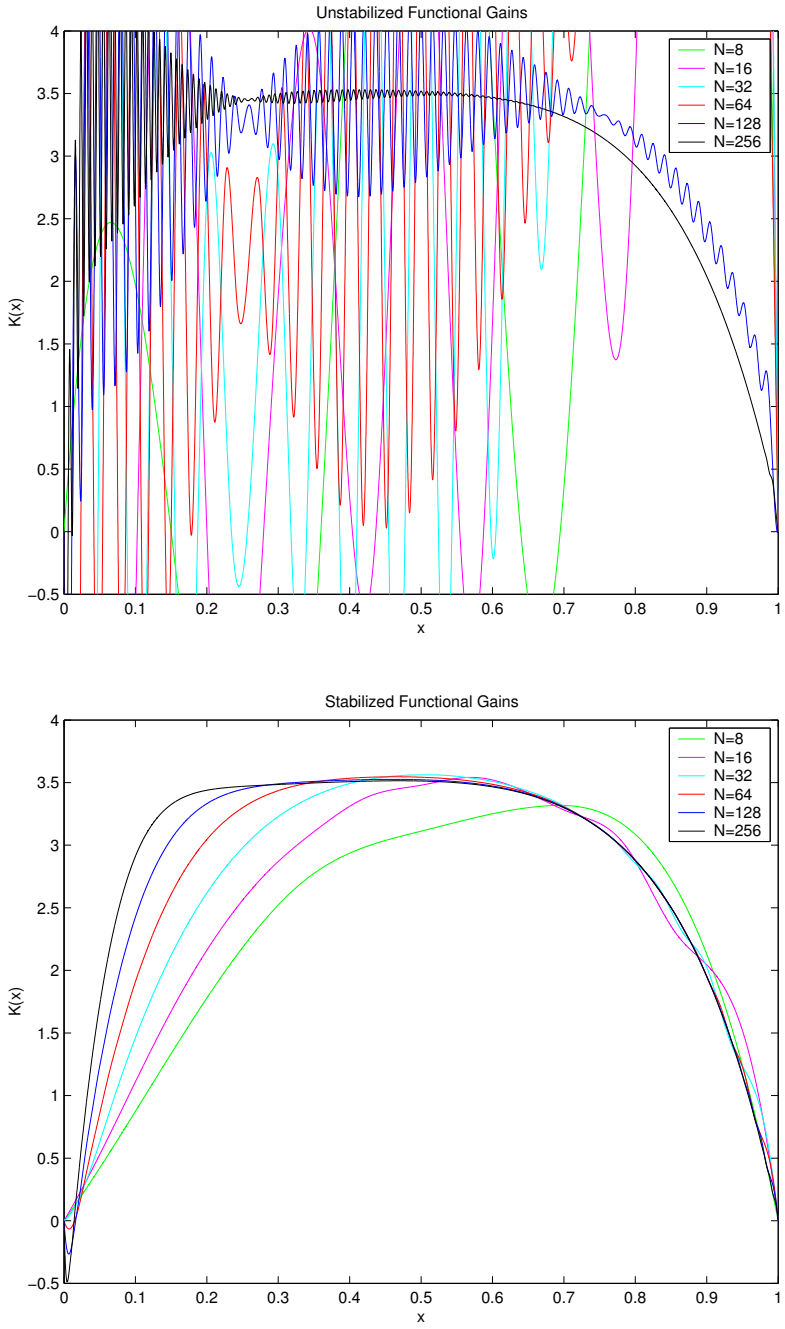

Figure 4.16: Epsilon = .0001, m = 4: Unstabilized and Stabilized Gains

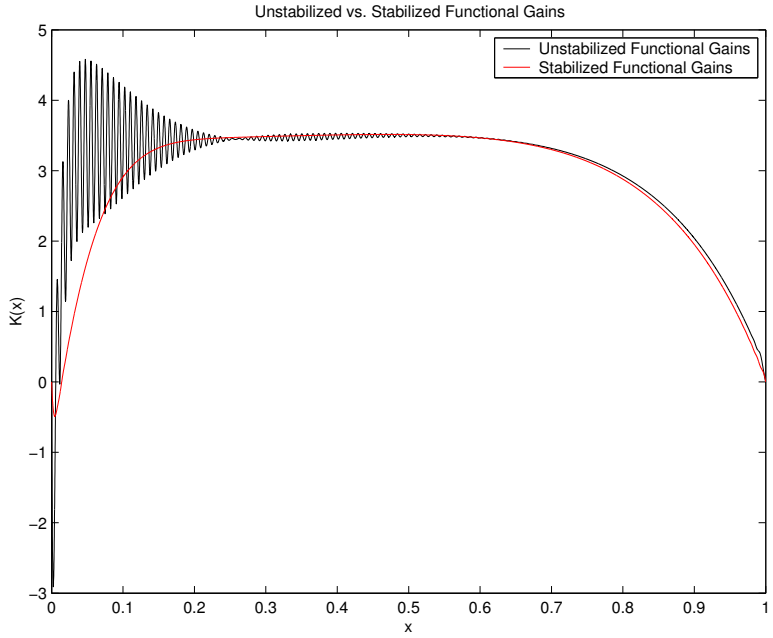

Figure 4.17: Epsilon = .0001, m = 4: Unstabilized versus Stabilized Gains, n = 256

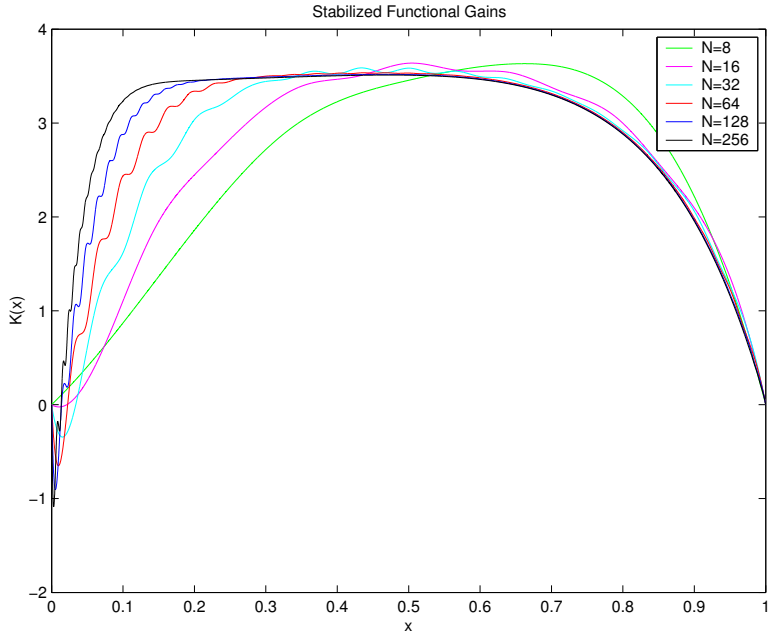

Figure 4.18: Epsilon = .0001, m = 8: Stabilized Gains

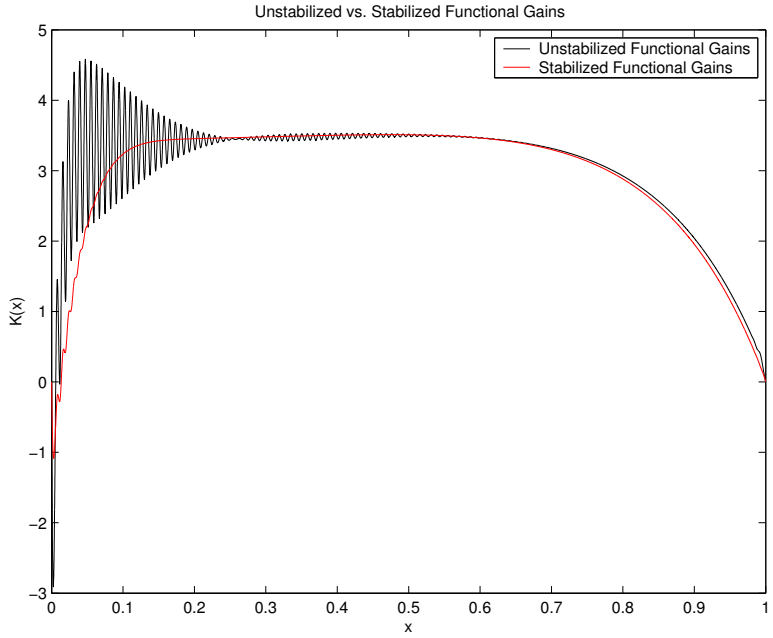

Figure 4.19: Epsilon = .0001, m = 8: Unstabilized versus Stabilized Gains, n = 256

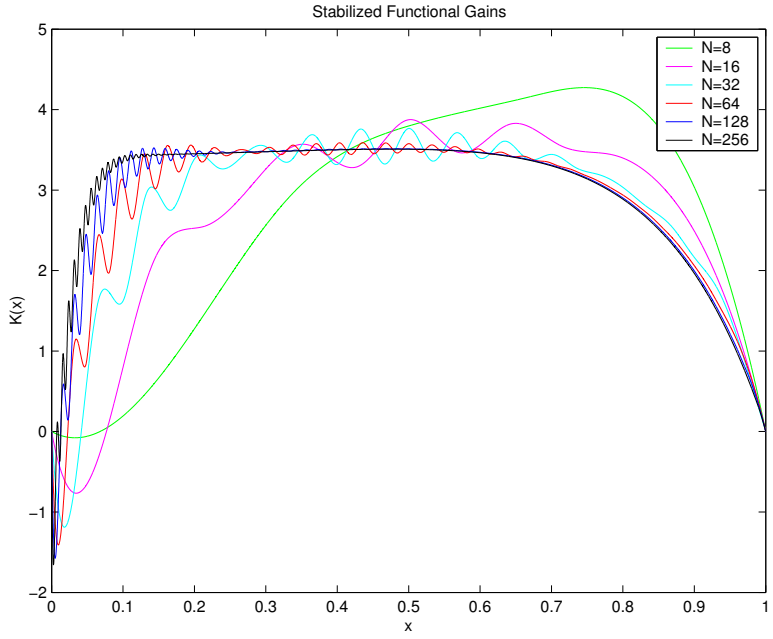

Figure 4.20: Epsilon = .0001, m = 16: Stabilized Gains

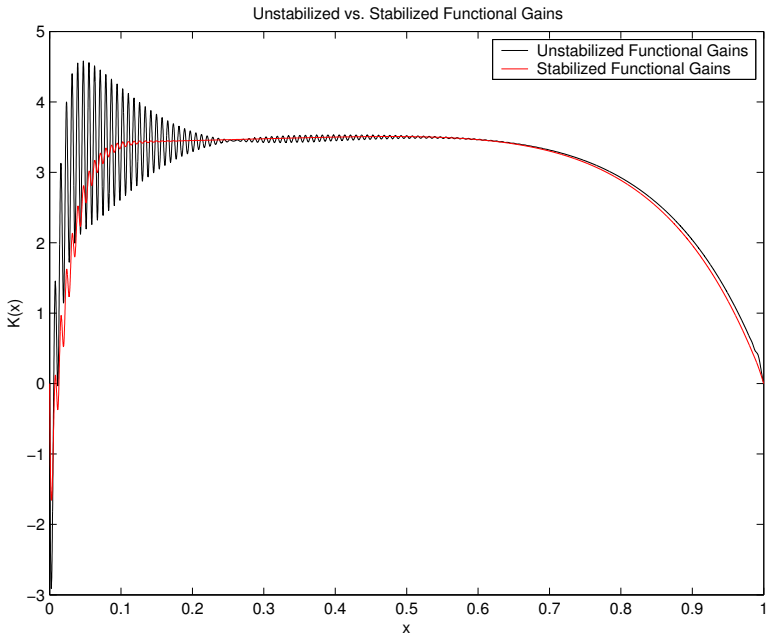

Figure 4.21: Epsilon = .0001, m = 16: Unstabilized versus Stabilized Gains, n = 256

4.1.5 Numerical Experiment 5: Limiting Case

We close with a few observations about the limiting control problem defined by the operator

$$[A_0\varphi(\cdot)](x) = -\kappa\frac{d\varphi(x)}{dx}, \qquad \text{for all} \quad \varphi(\cdot) \in \mathcal{D}(A_0), \tag{4.17}$$

where

$$D(A_0) = H_L^1(0,1) \triangleq \left\{\varphi(\cdot) \in H^1(0,1) : \varphi(0) = 0\right\}.$$

As indicated before, this system is used to guide the selection of the stabilization process. One can show that the LQR control problem for this system has a solution. It is tempting to use the GLS stabilization method to approximate this gain. One might expect that the limiting gain would look similar to the plots shown in Figure 4.22 where we set $\epsilon = .0001$ and $n = 800$. When $\epsilon = 0.0$, the unstabilized scheme fails to converge since the regular Galerkin finite element model does not satisfy POES as define by Banks and Kunisch in [8]. On the other hand, the stabilized GLS scheme converges. It seems reasonable that the limiting function in the bottom half of Figure 4.23 might be "close" to the functional gain for the control system defined by the convection operator (4.17) above. It would be interesting to study this problem in more detail. Finally, Figure 4.24 provides additional indication that the unstabilized gains are not converging.

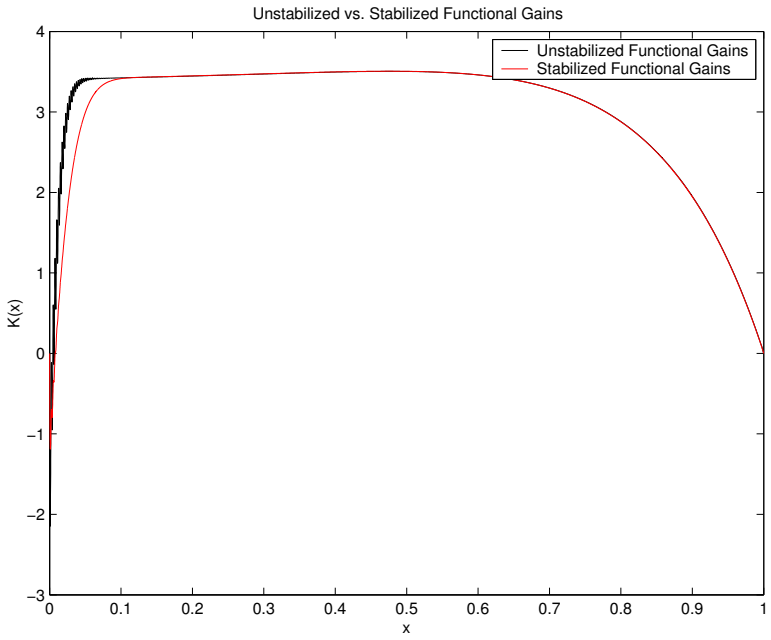

Figure 4.22: Epsilon = .0001, m = 8: Unstabilized versus Stabilized Gains, n = 800

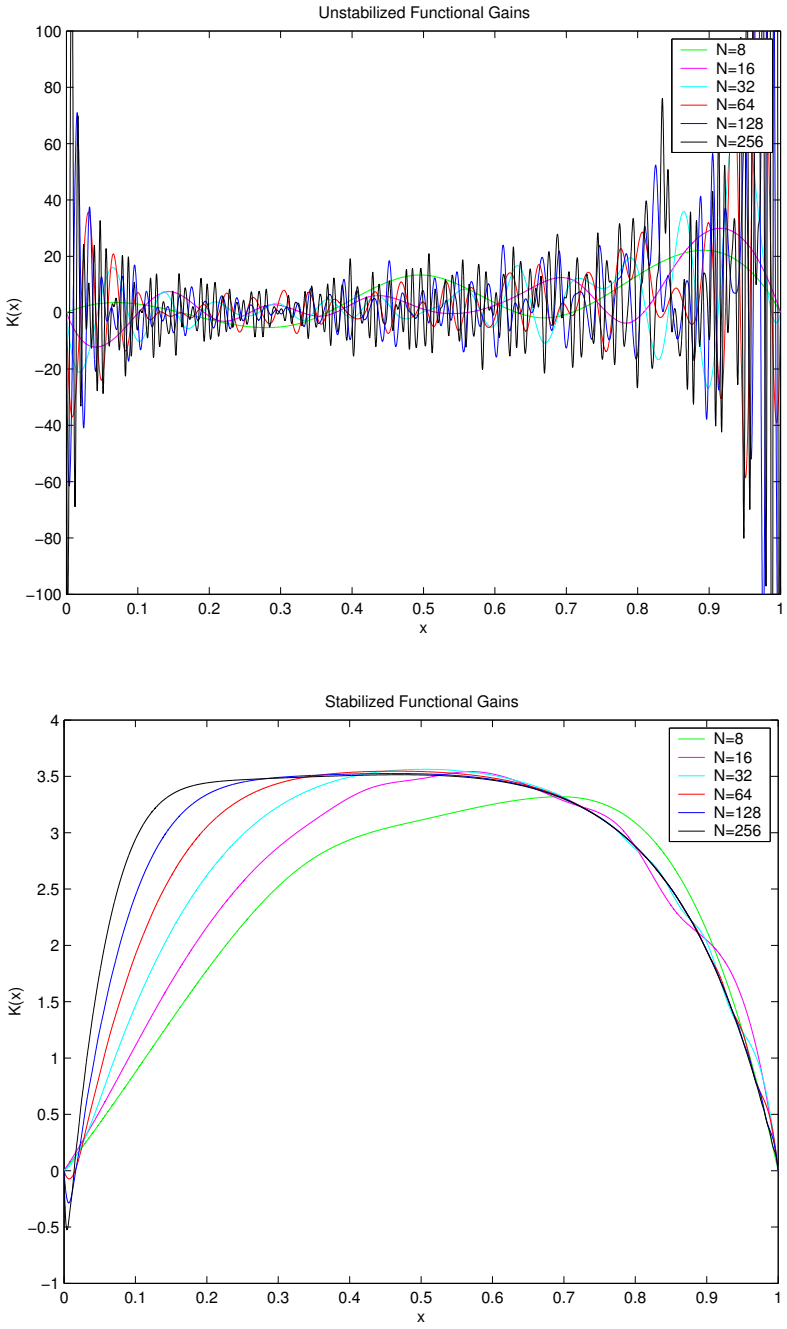

Figure 4.23: Epsilon = 0, m = 4: Unstabilized and Stabilized Gains

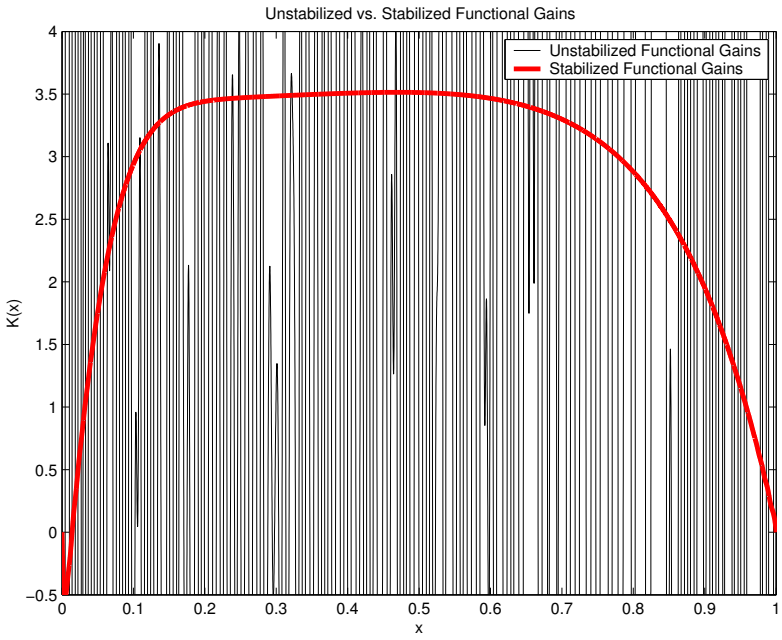

Figure 4.24: Epsilon = 0, m = 4: Unstabilized versus Stabilized Gains, n = 256

4.2 Conclusions and Directions for Future Research

In this thesis we investigated the application of the GLS stabilization method to the LQR control problem defined by convection diffusion equations. We conducted a careful numerical study of the impact that stabilization has on the convergence of the functional gains and the role that the stabilization parameter has on convergence and accuracy. The main findings and suggestions for further research may be summarized as follows:

1. In general, the GLS stabilized scheme produces much better approximations to the functional gains on coarse meshes. The positive effect of stabilization is more important as the Peclet number becomes large.

2. On fine meshes both schemes approach the true functional gain and the errors produced by the stabilized schemes mostly occur in the "boundary layer" where the functional gain has a large gradient. This is very similar to what occurs in the simulation problem due to the fact that the numerical dissipation may be too large.

3. If $Pe >> 1$, then it becomes important to choose a "good" stabilization parameter. In many cases the "optimal" parameter suggested by the error analysis for the steady problem is not a good choice for the control problem. Also, we discovered that using the limiting convection problem as a guide to help select the stabilization parameter may not be appropriate for the control problem. Therefore, it would be worthwhile to investigate methods for computing $\tau^n(m)$ as part of an adaptive algorithm.

4. Since the stabilized GLS scheme produces much better approximations on coarse grids, the GLS method can be used to generate an initial estimate for iterative methods on fine grids. This idea needs to be investigated further.

5. Although the numerical results imply convergence of the functional gains for the stabilized GLS method, we did not provide a proof of this conjecture. In order to prove convergence one must deal with the problem of dual convergence (since the convection diffusion problem is not self-adjoint) and show that the scheme satisfies POES as defined by Banks and Kunisch in [8]. This is more difficult for 2D and 3D problems

since, in these cases, the convection diffusion problem can not be transformed into a self-adjoint form.

6. Finally, more numerical experiments need to be done on 2D and 3D problems in order to see if stabilization might be useful for computing functional gains for flow control problems governed by linearized Navier-Stokes equations.

Bibliography

[1] V. Akcelik, G. Biros, O. Ghattas, K. Long, and B. Waanders. A variational finite element method for source inversion for convective-diffisive transport. *Finite Elements in Analysis and Design*, 39:683–705, 2003.

[2] E. Allen, J. A. Burns, D. Gilliam, J. Hill, and V. Shubov. The impact of finite precision arithmetic and sensitivity on the numerical solutions of partial differential equations. *Mathematical and Computer Modeling*, 35:1165–1195, 2002.

[3] J. A. Atwell and B. B. King. Stabilized finite element methods and feedback control for Burgers' equation. *Proceedings of the American Control Conference*, pages 2745–2749, June 2000.

[4] B. Bamieh. The structure of optimal controllers of spatially-invariant distributed parameter systems. *Proc. 36$^{\text{th}}$ IEEE Conf. on Decision and Control*, Dec. 8-12, 1997.

[5] B. Bamieh and M. Dahleh. Disturbance energy amplification in three-dimensional channel flows. *Proceedings of the American Control Conference*, pages 4532–4537, 1998.

[6] B. Bamieh and M. Dahleh. Energy amplification in channel flow with stochastic excitation. *Physics of Fluids*, 13:3258–3269, 2001.

[7] H. T. Banks and K. Kunisch. An approximation theory for nonlinear partial differential equations with applications to identification and control. *SIAM J. Control and Optimization*, 16:815–849, 1982.

[8] H. T. Banks and K. Kunisch. The linear regulator problem for parabolic systems. *SIAM J. Control and Optimization*, 22:684–698, 1984.

[9] A. Bensouussan, G. Da Prato, M. Delfour, and S. Mitter. *Representation and Control of Infinite Dimensional Syatems*. Birkhauser, Boston, 1993.

[10] T. R. Bewley. Flow control: New challenges for a new renaissance. *Progress in Aerospace Sciences*, 37:21–58, 2001.

[11] P. B. Bochev, M. D. Gunzburger, and J. N. Shadid. Stability of the SUPG finite element method for transient advection-diffusion problems. *Comput. Methods Appl. Mech. Engrg.*, 19:2301–2223, 2004.

[12] A. N. Brooks and T. J. R. Hughes. Streamline upwind/Petrov-Galerkin formulations for convection dominated flows. *Proceedings Third International Conference of Finite Element in Fluid Flows*, Canada, 1980.

[13] J. A. Burns. Non-linear distributed parameter systems with non-normal linearizations: Applications and approximations. *Research Directions in Distributed Parameter Systems*, R. C. Smith and M. A. Demetriou, Eds., SIAM Publications, Philadelphia:17–53, 2003.

[14] J. A. Burns and D. Arubio. A distributed parameter control approach to sensor location for optimal feedback control of thermal processes. *Proceedings of the 36th IEEE Conference on Decision and Control*, pages 2243–2247, 1997.

[15] J. A. Burns and S. Kang. A control problem for Burgers' equation with bounded input/output. *Nonlinear Dynamics*, 2:235–262, 1991.

[16] J. A. Burns and B. B. King. Optimal sensor location for robust control of distributed parameter systems. *Proceedings of the 33rd IEEE Conference on Decision and Control*, pages 3967–3972, 1994.

[17] J. A. Burns and B. B. King. A reduced basis approach to the design of low order feedback controllers for nonlinear continuous systems. *J. Vibrations and Control*, 4:297–323, 1998.

[18] J. A. Burns, B. B. King, D. Krueger, and L. Zietsman. Computation of feedback operators for distributed parameter systems with non-normal linearizations. *Proceedings of the American Control Conference*, pages 2083–2088, 2003.

[19] J. A. Burns, B. B. King, and Y. Ou. A computational approach to sensor/actuator location for feedback control of fluid flow systems. *Sensing, Actuation, and Control in Aeropropulsion, SPIE- The Society of Photo-Optimal Instrumentation Engineers Proceedings*, 2494:60–69, 1995.

[20] J. A. Burns and G. Peichl. On robustness and controllability for finite dimensional approximations of distributed parameter systems. *Proc. IMACS/IFAC Symposium on Distributed Parameter Systems, Hiroshema Japan*, October:491–496, 1987.

[21] S. S. Collis and M. Heinkenschloss. Analysis of the streamline upwind Petrov Galerkin method applied to the solution of optimal control problems. *CAAM Technical Report*, Submitted for publication, 2002.

[22] R. F. Curtain and H. Zwart. *An Introduction To Infinite-Dimensional Linear Systems Theory*. Springer-Verlag, New York, 1995.

[23] E. Dutra do Carmo and G. B. Alvarez. A new upwind function in stabilized finite element formulations, using linear and quadratic elements for scalar convection-diffusion problems. *Computer Methods in Applied Mechanics and Engineering*, 193:2383–2402, 2004.

[24] E. Dutro do Carmo and G. B. Alvarez. A new stabilized finite element formulations for scalar convection-diffusion porblems: the streamline and approximate upwind/petrov-galerkin method. *Computer Methods in Applied Mechanics and Engineering*, 192:3379–3396, 2003.

[25] C. A. J. Fletcher. *Computational Techniques for Fluid Dynamics, Volume 1*. Springer-Verlag, Berlin, 1991.

[26] M. Fortin. Finite element solution of the Navier-Stokes equations. *Acta Numerica*, 2:239–284, 1993.

[27] L. P. Franca and S. L. Frey. Stabilized finite element methods: II. The incompressible Navier-Stokes equations. *Computer Methods in Applied Mechanics and Engineering*, 99:209–233, 1992.

[28] L. P. Franca, S. L. Frey, and Thomas J. R. Hughes. Stabilized finite element methods: I. Application to the advective-diffusive model. *Computer Methods in Applied Mechanics and Engineering*, 95:253–276, 1992.

[29] A. C. Galeão and E. G. Dutra do Carmo. A consistent approximate upwind Petrov-Galerkin method for convection dominated problems. *Computer Methods in Applied Mechanics and Engineering*, 68:83–95, 1988.

[30] A. C. Galeão and E. G. Dutra do Carmo. Feedback Petrov-Galerkin methods for convection dominated problems. *Computer Methods in Applied Mechanics and Engineering*, 88:1–16, 1991.

[31] V. Girault and P.-A. Raviart. *Finite Element Methods for Navier Stokes Equations*. Springer-Verlag, New York, 1980.

[32] J. Hoepffner. *Control and Estimation of Wall Bounded Flow Systems*. PhD thesis, KTH, Stockholm, Sweden, 2004.

[33] M. Högberg, T. Bewley, and D. Henningson. Linear feedback control and estimation of transition in plan channel flow. *J. Fluid Mech.*, 481:149–175, 2003.

[34] H. Hu and H. Bau. Feedback control to delay or advance linear loss of stability in planer Poiseuille flow. *Proc. R. Soc. Lond. A.*, 447:299–312, 1994.

[35] T. J.R. Hughes, L. P. Franca, and G. M. Hulbert. A new finite element formulation for computational fluid dynamics: Viii. The Galerkin/least-squares method for advective-diffusive equations. *Computer Methods in Applied Mechanics and Engineering*, 73:173–189, 1989.

[36] T. J.R. Hughes, M. Mallet, and A. Mizukami. A new finite element formulation for computational fluid dynamics: Ii. Beyond SUPG. *Computer Methods in Applied Mechanics and Engineering*, 54:341–355, 1986.

[37] S. S. Joshi and J. L. Speyer J. Kim. Modeling and control of two dimensional poiseuille flow. *Proc. 34$^{\text{th}}$ IEEE Conf. on Decision and Control*, pages 921–927, 1995.

[38] M. R. Jovanovich and B. Bamieh. Modeling flow statistics using the linearized Navier-Stokes equations. *Proceedings of the 40th IEEE Conference on Decision and Control*, pages 4944–4949, 2001.

[39] M. R. Jovanovich and B. Bamieh. The spatio-temporal impulse response of the linearized Navier-Stokes equations. *Proceedings of the 2001 American Control Conference*, pages 1948–1953, 2001.

[40] M. R. Jovanovich and B. Bamieh. Input-output analysis of the linearized Navier-Stokes equations in channel flows. *Under consideration in J. Fluid Mech*, 2002.

[41] J. Douglas, Jr. and J. Wang. An absolutely stabilized finite element method for the Stokes problem. *Mathematics of Computation*, 52:495–508, 1989.

[42] B. B. King and D. A. Krueger. Burgers' equation: Galerkin least squares approximations and feedback control. *Mathematical and Computer Modelling*, 38:1075 –1085, 2003.

[43] J. L. Lions. *Optimal Control of Systems Governed by Partial Differential Equations*. Springer-Verlag, Berlin, 1971.

[44] M. A. Olshanskii. A low order galerkin finite element method for the navier-stokes equations of steady incompressible flow: a stabilization issue and iterative methods. *Computer Methods in Applied Mechanics and Engineering*, 191:5515–5536, 2002.

[45] A. Pazy. *Semigroups of Linear Operators and Applications to Partial Differential Equations*. Springer-Verlag, 1983.

[46] O. Pironneau. *Finite Element Method for Fluids*. John Wiley & Sons, Masson, 1989.

[47] P. M. Prenter. *Splines and Variational Methods*. John Wiley & Sons, New York, 1975.

[48] H.-G. Roos, M. Stynes, and L. Tobiska. *Numerical Methods for Singularly Perturbed Differential Equations*. Springer-Verlag, Berlin, 1991.

[49] L. N. Trefethen. Pseudospectra of linear operators. *SIAM Rev.*, 39:383–406, 1997.

[50] L. N. Trefethen, A. E. Trefethen, S. C. Reddy, and T. A. Driscoll. Hydrodynamic stability without eigenvalues. *Science*, 261:578–584, 1993.

[51] Frederic G. C. Valentin and Leopoldo P. Franca. Combining stabilized finite element methods. *Computational and Applied Mathematics*, 14:285–300, 1995.

[52] Eric D. Vugrin. *On Approximation and Optimal Control on Nonnormal Distributed Parameter Systems*. Ph.D. dissertation, Virginia Polytechnic Institute and State University, 2004.

Vita

Denise A. Krueger was born in Cincinnati, Ohio on July 22, 1962. She graduated from McAuley High School in Cincinnati, Ohio. In May 1984, she graduated from Xavier University with a Bachelor of Science in Mathematics. Upon graduation she accepted a position as a Cost Price Analyst for the Department of Defense at the AFPRO (Air Force Plant Representative Office)at General Electric in Cincinnati. After moving to Del Rio, TX she transferred to the Department of the Interior, in the capacity of Budget Analyst for the National Park Service, Amistad Recreation Area. As a stay at home mom for the next 12 years, she was actively involved in her children's education and activities. She began her graduate work at Virginia Tech in September, 1999, completing her Masters of Science in Mathematics in May, 2001 and Ph.D. in July 2004.